

Anonymous Referee #1

Interactive comment on “Estimates of micro-, nano-, and picoplankton contributions to particle export in the northeast Pacific” by B. L. Mackinson et al.

In this manuscript Mackinson et al. use phytoplankton pigments combined with large volume pump sampling, ^{234}Th deficiency measurements, and two sediment trap deployments to address the relative contributions of pico-, nano-, and microplankton to passive (sinking) carbon export in the northeast Pacific. This is an important topic, given the hypothesis proposed by Richardson & Jackson (2007) that production stemming from picoplankton may dominate the flux of particulate material in the ocean. To date, there have only been (to my knowledge) three published field studies specifically designed to address this hypothesis, thus this new dataset is quite valuable. There are some methodological issues with the authors' approach (as there will be with any approach to tackling this difficult problem) that I would like to see the authors address more directly and succinctly. However, I believe that this is a nice manuscript overall, and is certainly worthy of being published (with moderate revision). Below please find some major and minor issues that I believe should be dealt with:

Major Concerns:

There is no perfect way to address the contribution of picoplankton to particle export, because (1) there is no perfect way to measure export and (2) the source of the exported material is often obscured by grazing, aggregation, physical breakdown, and microbial remineralization processes. The authors have chosen to use a combination of ^{234}Th and pigments as their primary methods for this study. It is very important that they succinctly outline the problems with these methods:

1) ^{234}Th – The two primary methods for measuring vertical carbon fluxes in the field are ^{234}Th and sediment traps. Each has issues (hydrodynamic and degradation for sediment traps; steady-state assumptions and variable C: ^{234}Th ratios for ^{234}Th). For practical reasons, the authors rely very heavily on ^{234}Th measurements for this manuscript (although it is very nice that they have two sediment trap deployments that largely agree with the ^{234}Th -based results). Unfortunately, for their particular question ^{234}Th is inferior to sediment traps. It is incredibly important to note that, when determining the relative contributions of pico-, nano-, and microplankton to export using the authors' approach, the ^{234}Th measurements are COMPLETELY IRRELEVANT. The relative contribution of different size classes to export is completely determined by their pigment ratios in the >50-micron large-volume samples. This needs to be explicitly stated. The authors make the (defensible) assumption that these large particles (likely aggregates) collected by the pump at depth are representative of sinking material. As the authors note at the end of their discussion, however, the pumps do not sample fecal pellets effectively, and fecal pellets may both contribute significantly to export and represent different ratios of micro/nano/picoplankton than the aggregates sampled by the authors.

The reviewer correctly recognized that while the flux of ^{234}Th is required to determine the overall pigment flux, the relative contributions of pico-, nano-, and microplankton are, dependent only on the pigment ratios found on the $>53\text{-}\mu\text{m}$ particles. An explicit statement noting this has been added to the results section. In addition, we do acknowledge that the relative contributions of pico-, nano-, and microplankton to fecal pellet export likely differ from their relative contributions to algal aggregate export and noted that in our original manuscript (page 12648, lines 8 – 20).

2) Pigments – the other half of the authors' primary methodology is pigment analysis to determine the composition of the sinking material. There are a few issues with using pigments for this question (though nucleic acids, the other primary option, may have even greater issues). One issue that the authors have is that indicator pigments do not map perfectly into size classes. It would be nice to see the authors discuss the correlation between different pigments and size-fractionated chlorophyll. Another significant issue is differential pigment degradation. There is no a priori reason to assume that different indicator pigments are degraded at the same rate, especially when considering that picoplankton (primarily grazed by protozoans) and microplankton (largely grazed by mesozooplankton) likely undergo significantly different processes prior to being incorporated in aggregates or fecal pellets. C:pigment ratios may vary significantly with depth and inconsistently between taxa.

While it is true that pigments are not a perfect proxy for cell size, we did find a statistically significant correlation between microplankton pigment concentrations and the $> 5\text{-}\mu\text{m}$ size-fractionated chlorophyll concentrations for small-volume samples from the photic zone (page 12641, lines 18-20). We believe this justifies the use of indicator pigments as proxies for plankton size class for broad-level analysis.

Other Issues:

One of the strengths of this study is that the authors measured export and the contribution of pico-/nano-/microplankton at multiple stations and several different seasons. Given these measurements, it would be nice to see them discuss whether or not there are correlations between export and the contributions of pico/microplankton to surface biomass. Ultimately the Richardson & Jackson hypothesis is important because it pertains to the question of whether or not we would expect export to decrease in a more oligotrophic future ocean. In addition to looking directly at the proportion of picoplankton in export, the authors can also look at whether or not a picoplankton dominated ocean has less export than a microplankton dominated ocean.

No clear relationship was observed POC export, e-ratio, or NPP and the contribution of different phytoplankton size classes (as determined by pigment ratios) to integrated photic zone biomass. This is somewhat surprising, as the classical theory would suggest a strong correlation between microplankton pigments and e-ratio.

It would be nice to see the authors use pigment:carbon estimates to put together a

back-of-the-envelope calculation of the ratio of phytoplankton carbon: total carbon in the deep LV pump samples and sediment trap samples. Do the pigments that the authors measured comprise most of the organic carbon that is being exported or is a significant amount of the sediment trap material unaccounted for?

Following the reviewer's suggestion, Chl a:POC ratios were calculated for all in situ pump samples. Assuming that the shallowest samples (30 m) were comprised entirely of healthy phytoplankton, the amount of exported phytoplankton carbon (pigment supported carbon) can be estimated by multiplying this ratio by the Chl a concentration of deeper samples. Ratios phytoplankton carbon:total POC were calculated at 100 m (roughly the base of the photic zone) for all stations sampled. Results varied widely, ranging from 0.8% - 232% and averaging 69%.

On a similar note, although the authors do not give any methodological details for their fluorometric chlorophylls (this is an oversight that should be corrected – did they use the acidification method of Strickler & Parsons?) if they used the acidification method, they can get an estimate of phaeopigment concentration in the sediment trap as well. Although chlorophyll is not quantitatively converted to phaeopigments in mesozooplankton guts, phaeopigment concentration can still give an estimate of the proportion of flux that may be due to mesozooplankton fecal pellets and hence likely originating from microplankton but not showing up as microplankton indicator pigments.

Unfortunately, phaeopigment data is not available for the small-volume fluorometric chlorophyll samples. The in situ pump and sediment trap samples were analyzed by HPLC, which also did not yield phaeopigment data.

Since the authors talk about standing stocks sampled by SV and LV (and these two measurements do not agree) it is very important that they explicitly state when they are using standing stocks derived from SV or LV samples both in the text and in figures.

Standing stocks are always determined by integrating small-volume pigment concentrations over the photic zone due to our belief that these measurements more accurately reflect the community composition due to the pumps missing cells < 1 μm in size as noted in the original manuscript (page 12642, line 18 – 21). Explicit statements clarifying this have been added to the text.

Figure 8 shows microplankton indicator pigments often dominating even the 1-10 micron size fraction. This should probably be discussed since it clearly illustrates the issues with using phytoplankton pigments as indicators of size.

As noted earlier, the correspondence of indicator pigments with particular plankton size-classes is an imperfect one. Diatoms and dinoflagellates (as indicated by fucoxanthin and peridinin pigments) are counted as microplankton regardless of actual cell size. Given that significant numbers of small diatoms (< 5 μm) have been observed at OSP, it is not surprising to find microplankton pigments in the 1 – 10- μm size-fraction (Boyd and Harrison, 1999). However, for all cruises in this study, the highest

concentration of pigments was found in the 10 – 53- μ m size-class. The 1 – 10- μ m size-fraction generally represented a small percentage of overall pigments, and therefore, we do not feel the presence of microplankton indicator pigments in the 1 – 10- μ m size-fraction indicates a major flaw in our methodology. The presence of microplankton indicator pigments in the smallest size-fractions could also result from the collection of cell fragments or from the rupture of cells leading to a loss of material from larger screens during the pumping process. Finally, it should be noted that the presence of diatoms and dinoflagellates in the <53 size-fractions would lead to an underestimate of the small cell contribution to export.

This paper uses a lot of non-standard abbreviations. I would recommend that the authors add a table at the beginning of the manuscript that lists all their abbreviations so that readers don't have to hunt through the text to find out what mPF or PTh mean. Also, PTh is a strange choice for Th flux, since it could easily be mistaken to mean particulate thorium.

To address this, abbreviations have been defined at their first use in the text so the reader should not need to hunt for their definitions. Furthermore, P_{Th} is a common abbreviation for the loss rate of thorium on sinking particles while Th_P is typically used to represent particulate thorium (e.g. Coale and Bruland, 1985).

p. 12633 line 6 – Stukel & Landry 2010, and Lomas & Moran 2011 do not state that picoplankton export is proportional to biomass, but rather that its proportional contribution to export is less than to biomass, but still significant. Amacher et al. (2009, DSR I 56(12): 2206-2215) and Stukel et al. (2013, PinO 112-113: 49-59) should probably be cited as other studies that have attempted to directly assess the proportion of picoplankton in export. Amacher used nucleic acids and found a significant role for picos at ESTOC and Stukel used pigments and found a less than proportional role for picos in the Costa Rica Dome.

The relationship between biomass and export found by Stukel & Landry 2010, and Lomas & Moran 2011 has been corrected and the additional references have been added.

p. 12636 line 5 – Although there is nothing the authors can do about it at this point (and it probably isn't a huge problem), best practices with thorium involve an acidification step with HNO₃ to bring pH < 2 before spiking with the tracer Th-230 (Pike et al. 2005, Journal of Radioanalytical and Nuclear Chemistry 263(2) 355-360). This brings all the naturally particle-associated Th-234 into the dissolved phase so that it can equilibrate with the added Th-230. Without this step it is possible that the yield of Th-234 (initially bound to naturally occurring particles and colloids) and the yield of Th-230 tracer will be different. Also, no methods for yield analysis are mentioned.

The methods used in this study follow Buesseler et al. 2001 where there is no acidification. Previous studies by the Moran lab have consistently found ²³⁰Th recoveries

Mike 1/24/2015 9:21 PM

Comment [1]: What do you mean by leaching? Do you mean disruption of aggregates that are then retained on the smaller size class? If that is what you are referring to then you should use better wording.

Office 2004 Test Dri..., 1/24/2015 9:21 PM

Comment [2]: Agree with Mike. Or do you mean cell rupture and loss of organic matter?

"Leaching" really implies to chemically leach something – usually using a solvent, such as a mineral acid. As noted by Mike, I would not use this term.

of >95% for small volume samples using chemical separation and alpha counting. Furthermore, Moran lab results from the ²³⁴Th GEOTRACES Intercalibration experiment fell well within the group mean, indicating that acidification does little, if anything, to improve thorium recovery.

p. 12636 line 10 – “drying over” should be “drying oven”

The typo has been corrected.

p. 12636 line 25 - I do not see how mPF, nPF, and pPF are calculated. Is it simply the ratio of the summed indicator pigments that are believed to be responsible for each size class? This seems to be implied by Figure S2 which shows a 1:1 correlation between total indicator pigment and Chl a. This is not, however, the best way to estimate mPF, nPF, and pPF, since different taxa of phytoplankton will have different ratios of indicator pigment : Chl a. A better approach would probably be to multiply each indicator pigment by a pigment:C ratio for the taxa that it represents and then summing these carbon contributions (perhaps using a CHEMTAX approach – e.g. Mackey et al. 1996; MEPS 144: 265-283). Note that this should not change their primary results (the comparison of the proportions of picoplankton to biomass and export), but it would change the total proportion of picoplankton in biomass and export.

The indicator pigment PFs are calculated following the method outlined in Hooker et al. 2005. As the reviewer surmises, the indicator pigment concentrations for each size-class are summed and divided by the total indicator pigment concentration. While this is an admittedly simple approach, more complex methods (like CHEMTAX) still report taxonomic/size group data as a percentage of Chl a containing particles, and would still suffer from the issue of imperfect correlation between pigments and cell size. Furthermore, as the reviewer notes, the choice of method would not change the results of the comparison between contribution to biomass and contribution to export, which is the focus of this paper. Given this, we feel that our method is sufficient for this study.

The reviewer also suggested determining taxon-specific carbon export as a means for comparing the contributions of different phytoplankton size-classes to export. This paper is focused on pigment analysis and not on the determination of carbon export by different phytoplankton size-classes. We did not determine taxon-specific carbon in this study, and therefore, we are unable to calculate POC:pigment ratios. Given that POC:pigment ratios are strongly dependent on phytoplankton growth conditions, the use of literature values would be problematic. Given these complexities, an analysis of small cell carbon export is left for companion works.

p. 12643 line 23 – The authors have not stated how they determined ²³⁸U concentrations. Did they use the Owens et al. (2011 MarChem 127(1-4):31-39) or Chen et al. (1986, EarthPlanSciLett 80: 241-251) relationships or did they actually measure it directly?

The relationship established by Chen et al., 1986 was used in this study, following the method outlined by Baumann et al. 2013. A reference and statement clarifying this

Mike 1/24/2015 9:21 PM

Comment [3]: This method should reference Hooker et al. 2005 if it doesn't already. Clearly the reviewer is unfamiliar with this method if s/he is assuming what is done.

Brendan Mackinson 1/24/2015 9:21 PM

Comment [4]: Hooker et al. 2005 is referenced in the manuscript.

have been added to the text.

p. 12644 equation 1 – The equation shown neglects the effects of upwelling or downwelling which can (at times) lead to a significant error in simple thorium export models (see Savoye et al. 2006, MarChem 100(3-4): 234-249). Since the authors (like most who study thorium) have no way of estimating upwelling it is acceptable that they have neglected it, however, this term should definitely be included in equation 1 and the rationale behind ignoring it should be given.

Open ocean scavenging models typically do not include a term for vertical advection or do not distinguish between vertical and horizontal advection and diffusion for the reasons noted by the reviewer (e.g. Coale and Bruland, 1985, Charette et al. 1999.) Furthermore, vertical advection has been found to be important only in areas of high upwelling or downwelling velocity (Buesseler, 1998). The northeast Pacific is not a region known for strong upwelling or downwelling.

p. 12645 line 19 – “decreasee” should be “decrease”

The typo has been corrected.

p. 12645 line 25 – the POC/234Th ratio in traps is substantially higher than the ratio of particles collected by pumps. This is significant since it suggests that there may be a substantial amount of sinking material that is not being collected by the pumps. Such a situation could arise if there is a rapidly sinking particle fraction (perhaps fecal pellets) that has a high C:Th ratio that is similar to the higher bulk C:Th ratio found in surface water as well as a slowly sinking particle fraction that has time to equilibrate with lower bulk C:Th ratios at depth. This should be discussed as it bears on the question of whether or not the pump samples pigment ratios are representative of all sinking material.

We agree that the collection of a rapidly sinking particle fraction (fecal pellets) by the traps and not the pumps is a plausible explanation for the differing POC:Th ratios between the two methods and comment on this at length in the discussion section. The higher POC:Th and POC:Pigment ratios observed in the material collected by the traps relative to material collected by the in situ pumps implies that a significant proportion of the exported material could be carbon-rich, pigment-depleted fecal pellets.

p. 12646 line 4 – I cannot find a Fig. 11c

The typo has been corrected. The figure being referred to was Fig. 12c.

p. 12648 lines 15-20 – the authors point out that much of picoplankton production will be grazed and that the grazing pathway will not show up with their methodology. This is true. However, they then suggest that this may lead to an underestimate of the role of picoplankton by their methodology. This is not true. While picoplankton can certainly be exported by grazing pathways, they are most likely exported after transfer through one (or two) protozoan grazing steps which will degrade a significant fraction of their carbon

before the protozoans are grazed by large fecal pellet-producing mesozooplankton. Microplankton, by contrast are much more likely to be grazed directly by mesozooplankton, hence contributing a significantly greater fraction of their biomass to export. Thus the grazing pathway (which was not assessed by the methodology used by the authors) is actually much more likely to underestimate the contribution of microplankton than picoplankton. This is particularly important since, as the authors note at the end of the discussion, fecal pellet export is substantially greater than algal aggregate export in their study region.

As the reviewer noted, the classic paradigm for carbon export suggests that large phytoplankton are grazed by mesozooplankton leading to efficient export via fast sinking fecal pellets while smaller plankton are grazed by microzooplankton, leading to less efficient export and enhanced recycling through the microbial loop. However, in the northeast Pacific mesozooplankton are known to be omnivorous and are not thought to exhibit a strong grazing control on large phytoplankton such as diatoms, which are instead subject to bottom-up control due to iron limitation (Stoecker and Capuzzo, 1990, Dagg, 1993, Gifford, 1993, Goldblatt, et al. 1999, Harrison, 2002). Direct sinking is therefore a more likely fate for diatoms and other large phytoplankton. In contrast, small phytoplankton are tightly controlled by grazing in the northeast Pacific and are thus less likely to sink directly. In addition, recent studies have shown that indirect export can be an important pathway for small cell export due to grazing of individual pico- and nanoplankton by salps and grazing of small cell aggregates by mesozooplankton such as copepods (Richardson et al., 2004; Richardson and Jackson, 2007; Stukel and Landry, 2010).

Table 1 – I find this table to be slightly confusing. It might be easier to read if there were borders around the cells to show which samples go with which cruises.

Horizontal borders have been added between cruises in order to clarify which samples correspond to which cruise.

Table 2 – Please define all abbreviations so readers don't have to hunt through the text.

All abbreviations have been defined at their first use in the text and in the captions of figures and tables.

Figure 2 – I would recommend only showing plots down to 200 m (since I believe that is the deepest depth of the authors' samples) in the interest of making upper water column patterns more visible.

Hydrography and ²³⁴Th activity data extends down to 500 m, and profiles were shown down to 300 m in an effort to show upper water column data clearly while still showing the ²³⁴Th/²³⁸U activity ratio reaching/approaching ~1 at depth, indicating secular equilibrium.

Figure 9 – This is an important figure with a lot of data crammed into it. Is it possible to

make it a bit larger so that patterns are more visible?

The figure is already at the maximum size permitted by the journal. Data for the figure is also included in the appendices.

Figure 10 - legend and figure, there is no symbol for Harrison, 2002

As noted in the figure caption, NPP data from Harrison, 2002 and POC fluxes from Wong et al., 1999 are combined as one data point. The symbol has been moved in between Wong et al., 1999 and Harrison, 2002 in the figure legend in an effort to reduce confusion.

Anonymous Referee #2

Interactive comment on “Estimates of micro-, nano-, and picoplankton contributions to particle export in the northeast Pacific” by B. L. Mackinson et al.

GENERAL COMMENTS

Topic of this paper ‘contributions of nano- and picoplankton to export flux’ is an interesting and important topic. Quantitative study on this issue is still limited in marine ecosystems, although this is not the first paper to deal with this issue. Thus, present paper is worth being published in Biogeosciences. However, I have some points which need to be addressed before publishing on BG. Especially, authors need to make more suitable and careful discussion on 1) accuracy of the conclusion from this study, 2) possible underestimation of contribution of nanopicoplankton to export flux, and 3) conversion factors of Chlorophyll a to POC for micro- nano- picoplankton in this study area.

SPECIFIC COMMENTS

INTRODUCTION

It is better if authors could clearly point out their study purpose.

The purpose of the study as stated in the introduction is to “build upon prior investigations of phytoplankton community composition and export production along Line P by examining the distributions of organic carbon, phytoplankton indicator pigments, and ²³⁴Th in three particle size-fractions,” (p. 12634, line 4-6).

P. 12634 L.9-12: Authors can not say like that since authors do not show any data on chlorophyll a-carbon ratio for micro-, nano- and picoplankton.

The focus of this paper is on pigment analysis and taxon-specific carbon was not determined in this study, and therefore, we are unable to calculate POC:pigment ratios. However, pigment concentration is commonly used as a proxy for biomass. “POC export” has been edited to read “particle export” in the passage noted by the reviewer to avoid confusion.

DISCUSSION

P.12648 L27-29: ‘zooplankton grazing and cell degradation’ may also contribute to POC loss. Then, this sentence is not suitable to explain the low pigment and high POC in the trap compared to pumping.

We do not feel that acknowledging a possible source of error in the methodology, that grazing and cell degradation within the trap tube could slightly reduce the pigment concentration of trap samples over the 3-day deployment, invalidates the observed trends.

CONCLUSIONS

P.12649 L23-25: Do authors want to say their methodology is not reliable to quantify contribution of micro- nano- picoplankton to the export flux, and finally authors have wrong data

set? If this is the case, this paper is totally useless.

Once again, we do not feel that acknowledging a sampling bias invalidates the results of the study. However, given the sampling bias and the fact that our methodology did not account for all pathways of export, we do not believe that our results disprove the hypothesis put forth by Richardson and Jackson (2007).

P. 12650 L2-16: Authors should show and discuss conversion factors of Chlorophyll a to POC for micro- nano- picoplankton in this study area. Contribution of each phytoplankton category to 'POC' export can be changed due to the factors.

As stated previously, taxon-specific POC:pigment ratios could not be calculated in this study. Given that POC:pigment ratios are strongly dependent on phytoplankton growth conditions, the use of literature values would be problematic. However, by comparing pigment fluxes with pigment standing stocks it is possible to estimate how efficiently cells of different size-classes are exported from surface waters. While this is by no means the only factor influencing POC export, it does suggest the relative contributions phytoplankton of different size-class make to the biological pump via aggregation and sinking.

Estimates of micro-, nano-, and picoplankton contributions to particle export in the northeast Pacific

B. L. Mackinson¹, S. B. Moran¹, M. W. Lomas², G. M. Stewart³, R. P. Kelly¹

[1] {Graduate School of Oceanography, University of Rhode Island, Narragansett, RI 02882, USA}

[2] {Bigelow Laboratory for Ocean Sciences, East Boothbay, ME 04544, USA}

[3] {Queens College and Graduate Center, City University of New York, Flushing, NY 11367, USA}

Correspondence to: B. L. Mackinson (bmackinson@my.uri.edu)

Abstract

The contributions of micro-, nano-, and picoplankton to particle export were estimated from measurements of size-fractionated particulate ^{234}Th , organic carbon, and phytoplankton indicator pigments obtained during five cruises between 2010 and 2012 along Line P in the subarctic northeast Pacific Ocean. Sinking fluxes of particulate organic carbon (POC) and indicator pigments were calculated from ^{234}Th – ^{238}U disequilibria and, during two cruises, measured by sediment trap at Ocean Station Papa. POC fluxes at 100 m ranged from 0.65 – 7.95 $\text{mmol m}^{-2} \text{d}^{-1}$, similar in magnitude to previous results at Line P. Microplankton pigments dominate indicator pigment fluxes (averaging $69 \pm 19\%$ of total pigment flux), while nanoplankton pigments comprised the majority of pigment standing stocks (averaging $64 \pm 23\%$ of total pigment standing stock). Indicator pigment loss rates (the ratio of pigment export flux to pigment standing stock) point to preferential export of larger microplankton relative to smaller nano- and picoplankton. However, indicator pigments do not quantitatively trace particle export resulting from zooplankton grazing, which may be an important pathway for the export of small phytoplankton. These results have important implications for understanding the magnitude and

31 mechanisms controlling the biological pump at Line P in particular, and more generally in
32 oligotrophic gyres and high-nutrient, low-chlorophyll regions where small phytoplankton
33 represent a major component of the autotrophic community.

34

35 1 Introduction

36 Phytoplankton community structure exerts an important influence on the strength and
37 efficiency of the biological pump (Michaels and Silver, 1988; Boyd and Newton, 1999; Thibault
38 et al., 1999; Brew et al., 2009; Lomas and Moran, 2011). Small nano- and picoplankton
39 dominate the phytoplankton community in the oligotrophic gyres and high-nutrient, low-
40 chlorophyll (HNLC) oceanographic regions. It has traditionally been thought that small
41 phytoplankton represent a relatively small fraction of the downward flux of particulate organic
42 carbon (POC) relative to larger phytoplankton, such as diatoms, which are generally thought to
43 contribute disproportionately to POC export (e.g., Michaels and Silver, 1988). Recent studies
44 have challenged this idea, suggesting that small phytoplankton contribute significantly to POC
45 export, possibly through aggregation and incorporation into fecal pellets (Richardson and
46 Jackson, 2007; Amacher et al., 2009; Stukel and Landry, 2010; Lomas and Moran, 2011; Stukel
47 et al., 2013). A better understanding of the controls on the relative importance of small
48 phytoplankton in POC export is needed to refine our understanding of the magnitude and
49 mechanisms controlling the biological pump, particularly as recent climate models predict an
50 expansion of the oligotrophic gyres where small cells dominate (Irwin et al., 2006; Polovina et
51 al., 2008; Morán et al., 2010).

52 Ocean Station Papa (OSP, 50°N, 145°W), the site of one of the longest-running ocean
53 time-series, is located in the northeast Pacific Ocean in one of three major HNLC regions.
54 Previous attempts to resolve the apparent paradox of low phytoplankton biomass and high nitrate
55 concentrations at OSP concluded that a bottom-up control related to iron limitation is most
56 important for large phytoplankton (Muggli et al., 1996; Harrison, 2006; Marchetti et al., 2006),
57 while microzooplankton grazing exerts a strong top-down control on pico- and nanoplankton
58 (Landry et al., 1993; Harrison et al., 1999; Rivkin et al., 1999). Primary production at the
59 stations proximal to the coast on Line P (P4 & P12) is not iron-limited and diatom blooms are
60 typically observed in spring and late summer (Boyd and Harrison, 1999; Thibault et al., 1999).
61 At the offshore stations (including OSP) the phytoplankton community is dominated by cells <5-

Brendan Mackinson 1/17/2015 2:36 PM
Deleted: in proportion to their contribution
to biomass

64 μm and the seasonal variability of primary production is relatively low ($\sim 25 \text{ mmol C m}^{-2} \text{ d}^{-1}$ in
65 winter and $\sim 67 \text{ mmol C m}^{-2} \text{ d}^{-1}$ in summer) (Boyd and Harrison, 1999; Thibault et al., 1999;
66 Choi et al., 2014). In contrast to the low variability in primary production, POC export recorded
67 by moored sediment traps at OSP exhibits a stronger seasonal cycle with fluxes at 200 m depth
68 ranging from $\sim 0.4 \text{ mmol C m}^{-2} \text{ d}^{-1}$ in winter to $\sim 2.4 \text{ mmol C m}^{-2} \text{ d}^{-1}$ in summer (Timothy et al.,
69 2013). The average annual sediment trap POC flux at OSP ($1.4 \pm 1.1 \text{ mmol C m}^{-2} \text{ d}^{-1}$) is nearly
70 five times lower than the annual net community production (ANCP) at OSP ($6.3 \pm 1.6 \text{ mmol C}$
71 $\text{m}^{-2} \text{ d}^{-1}$), suggesting that the majority of organic carbon export is due to active transport by
72 zooplankton and/or dissolved organic carbon (DOC) export (Timothy et al., 2013; Emerson,
73 2014).

74 This study builds upon prior investigations of phytoplankton community composition and
75 export production along Line P by examining the distributions of organic carbon, phytoplankton
76 indicator pigments, and ^{234}Th in three particle size-fractions. Sinking fluxes of POC and
77 indicator pigments from the upper waters ($\sim 100 \text{ m}$) were calculated from the ^{234}Th – ^{238}U
78 disequilibrium and, during two cruises, measured at OSP using free-floating sediment traps. A
79 comparison of indicator pigment fluxes with the respective standing stocks suggests that
80 microplankton (20 – 200- μm) make up a higher percentage of particle export than biomass,
81 whereas pico- and nano plankton (0.2 – 2- μm and 2 – 20- μm) make up a lower percentage of
82 particle export than biomass.

Brendan Mackinson 1/25/2015 3:27 PM
Deleted: POC

Brendan Mackinson 1/25/2015 3:27 PM
Deleted: POC

84 2 Methods

85 2.1 Study location

86 Sample collection was conducted at five stations along Line P (P4, P12, P16, P20, and
87 P26 (OSP)) during cruises aboard the *CCGS John P. Tully* in August 2010, February 2011, June
88 2011, February 2012, and June 2012 (Fig. 1, Table 1). Line P is located at the southern edge of
89 the Alaskan Gyre, and the prevailing winds and surface currents are west-east (Bograd et al.,
90 1999). Because precipitation and continental run-off exceed evaporation, a permanent halocline
91 exists at $\sim 100 \text{ m}$ impeding deep winter mixing. In addition, a seasonal thermocline forms at ~ 50
92 m in spring and shoals to $\sim 20 \text{ m}$ in summer (Freeland et al., 1997; Thibault et al., 1999;
93 Freeland, 2013; Timothy et al., 2013).

97 2.2 Net primary production by ^{14}C incubation

98 Rates of net primary production (NPP) were determined following the protocols outlined
99 in Lomas et al. (2012). Samples were collected with Niskin bottles from seven depths in the
100 euphotic zone corresponding to 1, 5, 9, 17, 33, 55, and 100% of surface irradiance. Three ‘light’
101 bottles, a single ‘dark’ bottle, and a single initial (T_0) bottle were each spiked with $\sim 10\ \mu\text{Ci}$
102 $\text{NaH}^{14}\text{CO}_3$. A sub-sample to confirm total added activity was removed from the T_0 bottle at each
103 light depth and immediately added to an equal volume of β -phenylethylamine. Bottles were
104 incubated under simulated in situ conditions, using neutral density screening to mimic light
105 levels at the depth of sample collection, in an on-deck incubator for ~ 24 hours. After incubation,
106 125 mL sub-samples from each light and dark bottle were filtered through an Ahlstrom 151 (0.7-
107 μm nominal pore size) and a Whatman Track Etch 5- μm filter and rinsed with 10% HCl.
108 Samples were counted on a Perkin Elmer TriCarb 2900LR ~ 48 h after the addition of 5 mL of
109 Ultima Gold (Perkin Elmer, USA) scintillation cocktail.
110

111 2.3 Water column ^{234}Th

112 Total ^{234}Th (dissolved + particulate) analysis followed the procedures outlined in Bauman
113 et al. (2013). Briefly, samples (4 L) were collected by Niskin bottle at 12 depths (surface to
114 ~ 500 m) and spiked with ^{230}Th to monitor Th recovery. Samples were then treated with 7-8
115 drops of concentrated NH_4OH solution, followed by 25 μL of 0.2 M KMnO_4 , and finally with
116 11.5 μL of 1.0 M MnCl_2 to form a MnO_2 precipitate that quantitatively scavenges Th (Benitez-
117 Nelson et al., 2001; Buesseler et al., 2001; van der Loeff et al., 2006). After 1 hour, samples
118 were vacuum filtered onto 25 mm glass microfiber filters (GM/F, 1- μm nominal pore size) that
119 were frozen for later analysis in the shore-based laboratory. To prepare samples for counting,
120 filters were dried at 50°C for ~ 24 hours, mounted on acrylic planchets, and covered with
121 aluminum foil. To quantify ^{234}Th , the beta emission of $^{234\text{m}}\text{Pa}$ ($E_{\text{max}} = 2.19\ \text{MeV}$; $t_{1/2} = 1.2\ \text{min}$)
122 was counted using a RISØ National Laboratory low-background beta detector (Roskilde,
123 Denmark). Each sample was counted four times over a period of approximately six half-lives,
124 with the first count made at least 10 days after collection to allow for the decay of short-lived
125 isotopes, and the final count used to quantify background levels. Data were fitted to the ^{234}Th
126 decay curve to calculate the decay-corrected activity at the time of sample collection. Following
127 the ^{234}Th analysis, Th was radiochemically purified and ^{230}Th was measured by alpha particle

emission in order to determine scavenging efficiency. Small-volume scavenging efficiencies were found to be >90%. ^{238}U activities were calculated from salinity using the relationship $^{238}\text{U} = 0.07081 \times S (\text{‰})$ (Chen et al., 1986)

2.4 Water column POC, Chl *a*, and indicator pigments

Water samples for POC, Chl *a*, and phytoplankton indicator pigments were collected from the same depths in the photic zone as for NPP samples. Suspended POC was measured on 1 L seawater samples filtered onto pre-combusted Ahlstrom 151 filters and frozen at -20°C until analysis. Samples were dried at 60°C in a drying oven, fumed in a desiccator containing concentrated hydrochloric acid for 24 h to remove inorganic carbonates, and dried again at 60°C. Samples were then analyzed on an EA-440 Analyzer (Exeter Analytical, Inc., Chelmsford, MA) (Pike and Moran, 1997). Chl *a* samples were analyzed using the methods outlined in Lomas et al. (2012). Separate samples (~0.2 L) were filtered onto Ahlstrom 151 and 5-μm Whatman Track Etch polycarbonate filters and frozen at -20°C until analysis. Samples were then extracted in 5 mL of 90% acetone for 24 h at -20°C and analyzed using a calibrated TD-700 fluorometer.

Indicator pigment samples were collected on separate Ahlstrom 151 filters and stored at -80°C until analysis by high-performance liquid chromatography (HPLC) at the Bermuda Institute of Ocean Sciences in the Bermuda Atlantic Time-series Study Laboratory (Knap et al., 1997). Fucoxanthin (FUCO), peridinin (PER), 19'-hexanoyloxyfucoxanthin (HEX), 19'-butanoyloxyfucoxanthin (BUT), alloxanthin (ALLO), total chlorophyll *b* (TChl *b*), and zeaxanthin (ZEA) were analyzed as indicator pigments based on their correspondence to particular phytoplankton taxonomic groups. Indicator proportion factors (PFs) were calculated to further analyze the size-distribution of the phytoplankton community (Hooker et al., 2005; Lomas and Moran, 2011). The sum of FUCO and PER concentrations was used to determine the microplankton proportion factor (mPF), while the sum of HEX, BUT, ALLO, and TChl *b* was used to determine the nanoplankton proportion factor (nPF), and ZEA was used to determine the picoplankton proportion factor (pPF) (Hooker et al., 2005; Lomas and Moran, 2011). Hooker et al. (2005) included TChl *b* in pPF, but because *Prochlorococcus* is not found in the study region, it was assumed in this study that any Chl *b* would be found in cells (e.g., chlorophytes and euglenophytes) in the nanoplankton size-class.

2.5 In situ pump sampling

Large-volume in situ pumps (Challenger Oceanic Systems and Services, UK and McLane Scientific, Falmouth, MA) were deployed for approximately four hours at depths of 30, 50, 100, 150, and 200 m. Each pump sampled 100 – 1000 liters to collect size-fractionated particles, with seawater passing sequentially through 53- μ m, 10- μ m, and 1- μ m Nitex screens. Particles were resuspended by ultrasonication in 0.7- μ m prefiltered seawater and filtered onto separate pre-combusted GF/F filters for parallel analysis. Indicator pigment samples were stored at -80°C until analysis by high-performance liquid chromatography (HPLC) at the Bermuda Institute of Ocean Sciences in the Bermuda Atlantic Time-series Study Laboratory (Knap et al., 1997). Filters for analysis of POC and ^{234}Th were frozen at -20°C until analysis. A sub-sample (~30% by weight) was cut with acetone-cleaned stainless steel scissors from each ^{234}Th filter for POC analysis, and these sub-samples were dried and fumed with concentrated HCl as described above. POC was then measured using a CE 440 CHN Elemental Analyzer (Exeter Analytical, Inc., Chelmsford, MA). The ^{234}Th filter subsample was dried at 60°C in a drying oven and counted on a RISØ beta detector as noted above.

2.6 Sediment trap sampling

Surface-tethered particle interceptor traps (PITS) with cylindrical tubes (KC-Denmark, Silkeborg, Denmark) were deployed for ~3 days at station P26 during the June 2011 and June 2012 cruises to collect particles at the depths of 30, 50, 100, 150, and 200 m. Due to limited wire-time and other cruise constraints it was not possible to deploy sediment traps at any other stations sampled as part of this study. The trap design and sampling procedure is described in Baumann et al. (2012). Four tubes (72 mm diameter, 450 mm length) were used at each depth, and tubes were filled with non-poisoned, 0.4- μ m filtered brine ($S = \sim 85 \text{ ‰}$) prior to deployment. Upon recovery trap brines were combined, particles were re-suspended and filtered onto pre-combusted GF/F filters, and swimmers were removed. Filters were stored frozen and later analyzed for POC, ^{234}Th , and indicator pigments as described above.

3 Results

3.1 Hydrography and NPP

Depth sections of temperature and density anomaly (σ_t) were generated using results from all CTD casts for a given cruise to improve horizontal data resolution (Fig. 2). The seasonal change in water temperature is largely confined to the upper ~100 m. Surface temperatures in August 2010 were ~14°C, while during the February cruises, surface temperatures were slightly cooler offshore (~6°C) than inshore (~8°C). During the June cruises, inshore temperatures were warmer (~10 – 12°C) while offshore temperatures remained relatively cool (~8°C). Density anomaly did not vary greatly between cruises below ~100 m. During the winter, a pool of less dense water (density of 1023 – 1025 kg m⁻³) was observed toward the coast (east of ~126°W). During the June cruises, this pool was observed extending west to ~130°W and during August 2010, it extended out to OSP (145°W). These data follow the expected seasonal pattern of a well-mixed water column in winter and increasing stratification moving from spring to summer.

Total NPP and >5- μ m size-fractionated NPP values were trapezoidally integrated over the euphotic zone (Table 2). A maximum total NPP of 91.9 mmol m⁻² d⁻¹ was measured at station P26 during June 2011, whereas the lowest value of 12.4 mmol m⁻² d⁻¹ was measured at station P26 during February 2012. These values agree to within a factor of two with the seasonal averages reported by Boyd and Harrison (1999). A maximum >5- μ m NPP of 39.6 mmol m⁻² d⁻¹ was at station P4 during June 2012 and a minimum of 2.2 mmol m⁻² d⁻¹ was measured at station P12 in February 2012.

3.2 Small- and large-volume POC concentrations

Suspended POC concentrations from Niskin bottle samples collected in the photic zone range from 1.1 – 7.1 μ mol L⁻¹. POC concentrations were generally lowest at the base of the photic zone, though decreasing concentrations with depth were not observed at all stations (Table S1). The highest suspended POC concentrations were measured at station P4 during all cruises. POC concentrations were also measured in three size-fractions of particles collected with large-volume in situ pumps (Table S2). Concentrations of each size-fraction tended to decrease with depth and were typically less than 0.5 μ mol L⁻¹ at all depths. One exception was at station P26 during February 2011 when POC concentrations at 30 m were between 1.8 and 2.9 μ mol L⁻¹ for all size-fractions.

219 The concentrations of POC collected using small-volume and large-volume methods
220 often do not agree for samples collected at the same location and depth (Gardner, 1977; Moran et
221 al., 1999; Liu et al., 2005; Liu et al., 2009). As reported in these previous studies, POC
222 concentrations measured by large-volume in situ pumps (summed for all size-fractions) are
223 significantly (ANOVA, $p < 0.05$) less than small-volume POC measurements from the same
224 station and similar depth (Fig. 3a). Explanations put forth to account for this discrepancy include
225 DOC adsorption to filters, pressure effects on particle retention in pump samples, the collection
226 of zooplankton by Niskin bottles but not pumps, and particle washout from pump filters (Moran
227 et al., 1999; Liu et al., 2005; Liu et al., 2009). In this study, the smallest pump size-fraction
228 was collected using a 1- μm Nitex screen, not a GF/F, resulting in the pumps missing the portion
229 of the POC on particles between 0.7- and 1- μm , which may further contribute to the difference
230 observed between the two methods. Lomas and Moran (2011) reported that sonication of in situ
231 pump samples to resuspend particles from the Nitex screens had no significant effect on
232 measured POC concentrations.

233

234 3.3 Particulate ^{234}Th and $\text{POC}/^{234}\text{Th}$ ratios

235 Size-fractionated particulate ^{234}Th activities in samples collected by in situ pump
236 generally decrease with depth, and are typically less than 0.1 dpm L^{-1} (Table S2). As with in situ
237 pump POC concentrations, station P26 during February 2011 is an exception, with values
238 exceeding 0.1 dpm L^{-1} for all size fractions at 30 m and throughout most of the water column for
239 the 1 – 10- μm fraction. Size-fractionated $\text{POC}/^{234}\text{Th}$ ratios (Fig. 4, Table S2) are less than ~ 6
240 $\mu\text{mol dpm}^{-1}$ for all size-classes at most stations, with higher values measured at stations P4 and
241 P12 in February 2012 and P4 in June 2012. $\text{POC}/^{234}\text{Th}$ ratios tend to decrease or remain constant
242 with depth, with one exception at station P12 during February 2012 where the maximum
243 $\text{POC}/^{234}\text{Th}$ was at 100 m for all size fractions. Also, the $\text{POC}/^{234}\text{Th}$ ratio does not vary greatly
244 between size-fractions (Fig. 4) as was observed in Speicher et al. (2006) and Brew et al. (2009).

245 The accuracy of ^{234}Th as a tracer of POC export depends on the assumption that ^{234}Th
246 and POC are sinking on the same particles, and therefore sinking at the same rate (Moran et al.,
247 2003; Smith et al., 2006; Speicher et al., 2006; Burd et al., 2007; Brew et al., 2009). A high
248 degree of correlation between the size-fractionated distributions of ^{234}Th and POC (Fig. 4) along
249 Line P provides evidence in support of this assumption. All correlations were statistically

significant ($p < 0.05$) and imply a strong coupling between particulate ^{234}Th and POC for all cruises. In addition, the clustering of data for the different size-fractions of particles (Fig. 4) indicates that in February 2012 the 10 – 53- μm size class contained the highest percentage of POC and particulate ^{234}Th , while the >53- μm size class contained the lowest percentage. In June 2012, the 1 – 10- μm size class had the lowest percentage of POC and particulate ^{234}Th while both the 10 – 53- μm and the >53- μm fractions contained higher percentages (Fig. 4).

3.4 Small-volume Chl *a* and indicator pigments

Concentrations of total Chl *a* and >5- μm Chl *a* measured by fluorometer (Table S1) were trapezoidally integrated over the photic zone to determine respective standing stocks. During August 2010, the >5- μm fraction accounted for >30% of the Chl *a* at all stations, with a maximum of 50% at station P26. During the other four cruises, the >5- μm size-fraction generally accounted for <30% of the total Chl *a*, except at station P26 in February 2012 and station P4 in June 2012. Previous studies have reported that larger cells are more abundant at stations closer to the coast (Boyd and Harrison, 1999), though this was not always apparent. The highest >5- μm percentage of Chl *a* was measured at station P26 during August 2010, June 2011, and February 2012. Phytoplankton indicator pigments and Chl *a* concentrations in samples from the euphotic zone samples were also measured by HPLC (Table S1). HPLC and fluorescence Chl *a* concentrations generally agreed to within a factor of two, and the correlation between the two measurements was statistically significant ($p < 0.05$) (Fig. S1). The correlation between the sum of the indicator pigment concentrations and the Chl *a* concentration was statistically significant ($p < 0.05$) and roughly 1:1, suggesting that the indicator pigments examined in this analysis accounted for most of the phytoplankton biomass (Fig. S2). Furthermore, the correlation between the >5- μm fraction of Chl *a* and mPF is statistically significant ($p < 0.05$), suggesting that this PF is a reasonable representation of that size-fraction of the phytoplankton community. Profiles of indicator pigment concentrations were trapezoidally integrated over the photic zone to quantify standing stocks (Table 3). FUCO was the most abundant microplankton pigment, and HEX was the most abundant nanoplankton pigment at most stations. Indicator pigment PFs (Fig. 5, Table S3) reveal that the phytoplankton community was typically dominated by nanoplankton, although at P4, and to a lesser extent at P20 in June 2012, microplankton pigments made up the bulk of the sample (~86% and ~52% respectively).

3.5 Large-volume size-fractionated Chl *a* and indicator pigments

Size-fractionated Chl *a* and indicator pigment concentrations were also measured by in situ pump (Table S4). Chl *a* was once again strongly correlated in a roughly 1:1 ratio with the sum of the indicator pigments ($p < 0.05$) (Fig. S3). The highest Chl *a* concentrations were measured in the 10 – 53- μm fraction during all cruises. In February 2012, the >53- μm fraction generally had the lowest concentrations, while in June 2012 and June 2011 the lowest concentrations were generally in the 1 – 10- μm fraction.

Ideally, small-volume and large-volume concentrations of Chl *a* and indicator pigments should agree for samples collected at the same station and depth, but this was not observed in this study (Fig. 3). Although differences between small- and large-volume measurements of POC have been reported (Gardner, 1977; Moran et al., 1999; Liu et al., 2005; Liu et al., 2009), few studies have compared Niskin bottle and in situ pump measurements of indicator pigments (Lomas and Moran, 2011). Relative to bottle samples, the pump samples indicate higher concentrations of microplankton pigments FUCO and PER and lower concentrations of ZEA and TChl *b*, which are pigments associated with pico- and nanoplankton (Fig. 3b-d). Large-volume pump and small-volume bottle measurements of the nanoplankton indicator pigments HEX, BUT, and ALLO generally agree within a factor of two (Fig. 3b-d). Given the small size of ZEA-containing *Synechococcus* and TChl *b*-containing chlorophytes and prasinophytes, it is likely that many of these cells pass through the 1- μm Nitex screen which would lead to under-sampling by the pumps (Liu et al., 2005). Bottles may undersample large, rare cells because the small volume might not be a statistically representative sample (Lomas and Moran, 2011). Furthermore, larger cells may settle below the spigot of the Niskin bottles, leading to a further bias against the collection of large cells (Gardner, 1977; Gundersen et al., 2001). Pumps sample higher concentrations of Chl *a* than bottles (Fig. 3a) at stations with high concentrations of Chl *a*, but when Chl *a* concentrations are low ($<200 \text{ ng L}^{-1}$), the pumps tend to undersample relative to the bottles.

Given these sampling differences, it is important to note that although the total concentrations (summed for all size-fractions) measured by the in situ pumps may be inaccurate, it is still possible that the >53- μm fraction accurately represents the composition of sinking particles. The disruption of loosely-bound aggregates during collection by the pumps could

cause an error in the >53- μm fraction, but this is considered unlikely due to the presence of nanoplankton (and in some cases picoplankton) pigments in this fraction. Furthermore, a recent study in the Sargasso Sea employed a similar methodology and also found picoplankton pigments in three particle size-classes, each >10- μm (Lomas and Moran, 2011).

Indicator pigment PFs calculated for the size-fractionated particles (Table S3) and plotted against depth (Figs. 6-8) reveal that while the overall indicator pigment concentrations vary with depth and across size-fractions, the PFs do not exhibit a systematic pattern of variation across size classes, depths, or seasons. The picoplankton pigment ZEA typically represents <10% of the total indicator pigments for all size classes. Microplankton pigments dominated samples at station P4 in February 2012 and June 2012, with mPFs typically exceeding 0.5 and 0.8, respectively, for each cruise. In addition, mPFs were high at station P26 during these times, with values generally exceeding 0.5 (Figs. 7-8). Nanoplankton pigments dominated at station P12 in February 2012 cruise with nPFs exceeding 0.5 for most samples. As with the small volume samples, FUCO was usually the most abundant microplankton pigment while HEX was usually the most abundant nanoplankton pigment (Table S4).

3.6 Total ^{234}Th , $^{234}\text{Th}/^{238}\text{U}$ activity ratios, and ^{234}Th fluxes

Total (dissolved + particulate) ^{234}Th activities, ^{238}U activities, and $^{234}\text{Th}/^{238}\text{U}$ activity ratios are listed in Table S5. Depth sections of these $^{234}\text{Th}/^{238}\text{U}$ activity ratios (Fig. 2d) indicate that areas of low $^{234}\text{Th}/^{238}\text{U}$ are prevalent in spring and summer and corresponding to periods known to have high particle export in this region (Wong et al., 1999; Timothy et al., 2013). ^{234}Th fluxes (P_{Th}) were calculated using these $^{234}\text{Th}/^{238}\text{U}$ results and a 2-D steady-state model of the radiochemical balance for ^{234}Th in the upper ocean,

$$\frac{\partial A_{Th}}{\partial t} = A_U \lambda_{Th} - A_{Th} \lambda_{Th} - P_{Th} + K_h \frac{\partial^2 A_{Th}}{\partial^2 x} + U_h \frac{\partial A_{Th}}{\partial x} \quad (1)$$

where A_U is the activity of ^{238}U , λ_{Th} is the ^{234}Th decay constant, A_{Th} is the activity of ^{234}Th , P_{Th} is the vertical flux of ^{234}Th on sinking particles, K_h is the eddy diffusion coefficient, and U_h is the current velocity (Coale and Bruland, 1985; Charette et al., 1999). Assuming a steady-state

($\partial A_{Th}/\partial t = 0$) over several weeks to months, and that the diffusive flux of ^{234}Th is small relative to advection and can therefore be ignored, the vertical flux of ^{234}Th (in $\text{dpm m}^{-2} \text{ d}^{-1}$) is defined by,

$$P_{Th} = \int_0^z \left[\lambda_{Th} (A_U - A_{Th}) + U_h \frac{\partial A_{Th}}{\partial x} \right] dz \quad (2)$$

where z is the depth of the water column over which the flux is measured. In this study, the gradient of thorium ($\partial A_{Th}/\partial x$) was only measured in the east-west direction (along Line P). Therefore, x is the east-west distance across which the gradient will be measured and U_h is the east-west current velocity. Current velocities determined from 5-year seasonal averages of surface drifter data (available from Fisheries and Oceans Canada) were found to be $6 \pm 4 \text{ cm s}^{-1}$ for the February cruises, $4 \pm 2 \text{ cm s}^{-1}$ for the June cruises, and $5 \pm 3 \text{ cm s}^{-1}$ for the August cruise. These values agree well with the $\sim 10 \text{ cm s}^{-1}$ value reported by McNally, (1981) and used by Charette et al., (1999). Given that the currents in the region generally flow west-east, and with no data at stations north and south of Line P, the north-south transport of ^{234}Th by advection had to be assumed to be negligible. At stations P12, P16, and P20, the ^{234}Th gradient was measured between the adjacent stations. For stations P4 and P26 (at either end of Line P), the gradient of ^{234}Th was determined from the adjacent station assuming a linear change extended beyond the measured transect.

^{234}Th fluxes (P_{Th}) calculated using the 2-D model are within 5% of fluxes determined using a steady-state 1-D model that ignores advection (Fig. S4). This indicates that, under these assumptions, the vertical flux of ^{234}Th on sinking particles is the dominant transport term. Consistent with previous studies, ^{234}Th fluxes at all stations were higher during the August and June cruises than during the February cruises (Fig. 9a) (Charette et al., 1999). Also, ^{234}Th fluxes did not exhibit a consistent trend along Line P.

3.7 ^{234}Th -derived POC fluxes

The $\text{POC}/^{234}\text{Th}$ ratio in the $>53\text{-}\mu\text{m}$ size-class and P_{Th} for a given depth horizon were used to calculate POC fluxes (P_{POC}) (Fig. 9). In most cases, P_{POC} decreases with depth, although in some cases, the maximum P_{POC} in a given profile occurs at 50 or 100 m. P_{POC} fluxes at 100 m range from $0.65 - 7.95 \text{ mmol m}^{-2} \text{ d}^{-1}$; they are generally higher in summer than winter, and

372 highest at station P4, consistent with previous studies at Line P (Charette et al., 1999; Wong et
373 al., 1999; Timothy et al., 2013).

374 The ratio of P_{POC} flux to NPP, referred to as the ThE -ratio, is an estimate of efficiency of
375 the biological pump (Buesseler, 1998). ThE -ratios determined using P_{POC} fluxes at the base of
376 the photic zone (Table 2, Fig. 10) are similar to those reported by Charette et al. (1999), and are
377 also in line with an annual average e -ratio determined using average sediment trap POC fluxes
378 (Wong et al., 1999) and annual average NPP (Harrison, 2002) (Fig. 10).

379

380 3.8 Sediment trap ^{234}Th and POC fluxes

381 The particle fluxes of both ^{234}Th and POC fluxes determined by the PITS traps (F_{Th} and
382 F_{POC} respectively) generally decrease with depth (Table 4). F_{Th} was higher in June 2012 than in
383 June 2011, though there was no clear difference between the two cruises for F_{POC} . A comparison
384 of the F_{Th} with the P_{Th} from corresponding stations and depths indicates that the F_{Th} is
385 consistently higher than the P_{Th} , though usually not by more than a factor of two. F_{POC} is also
386 consistently higher than P_{POC} , though again not by more than a factor of two (Fig. 11a). The
387 POC/ ^{234}Th ratios of particles caught in sediment traps (Table 9) tend to be slightly higher
388 (generally within a factor of 2) than the ratio of particles sampled by pumps at the corresponding
389 station and depth.

390

391 3.9 ^{234}Th -derived and sediment trap pigment fluxes

392 Sinking fluxes of Chl a (P_{Chla}) and indicator pigments ($P_{Pigment}$) were calculated from P_{Th}
393 and the Pigment/ ^{234}Th ratio measured on $>53\text{-}\mu m$ particles. Chl a and indicator pigment fluxes
394 (Table 3, Fig. 12a-c) are generally highest at station P4 and decrease moving offshore. The
395 highest indicator pigment fluxes were typically observed for microplankton pigments (FUCO
396 and PER) whereas the lowest were observed for the picoplankton pigment ZEA (Table 3, Fig.
397 12a-c). It is important to note that the differences between fluxes of different pigments at a given
398 station are determined by the pigment ratio on the $>53\text{-}\mu m$ particles and are independent of P_{Th} .

399 Sediment trap pigment fluxes ($F_{Pigment}$) were typically lower than $P_{Pigment}$ (Table 3, Fig.
400 11b). The maximum sediment trap fluxes of Chl a and most indicator pigments were determined
401 at 50 m in June 2011 and at 30 m in June 2012 (Table 3). For both deployments the deepest
402 fluxes were generally the lowest, presumably due to the progressive degradation of sinking

Brendan Mackinson 1/15/2015 9:55 PM
Deleted: e

phytoplankton and resulting loss of pigments. Chl *a* and indicator pigment fluxes were generally higher in June 2011 than in June 2012, which is the opposite of the trend observed for F_{Th} .

Pigment PFs determined for material captured by the PITS traps do not vary greatly with depth, suggesting that the quality of material sinking to depth is similar to that in the surface water, despite the general decrease of material (Figs. 6 and 8). Microplankton PFs are higher for trap samples than for bottle samples but not as high as for pump samples, while nPFs and pPFs are higher for trap samples than for pump samples but lower than for bottle samples.

4 Discussion

The results presented in this study build on previous investigations of export production in the northeast Pacific by providing estimates of the relative contributions of different phytoplankton size-classes to particle export. A comparison of indicator pigment standing stocks determined from small-volume samples and $P_{Pigment}$ fluxes suggests that while nanoplankton represented the bulk of phytoplankton biomass ($68 \pm 24\%$ of pigment standing stock, averaged for all stations and cruises), microplankton dominated the flux of pigmented material ($69 \pm 19\%$ on average) (Table 3, Fig. 12). Sediment trap pigment fluxes indicate a lower, but still substantial, relative contribution of microplankton to export, with microplankton pigments making up 47% and 33% of the total sediment trap indicator pigment flux in June 2011 and June 2012 respectively, as compared to 81% and 85% of total $P_{Pigment}$ fluxes. Though nano- and picoplankton did not form the majority of the algal aggregate flux, their $29 \pm 19\%$ contribution is significant and similar to contributions reported by Lomas and Moran (2011) for cyanobacteria and nano-eukaryotes in the Sargasso Sea.

Indicator pigment loss rates determined from both $P_{Pigment}$ fluxes and sediment trap pigment fluxes imply that microplankton are exported more efficiently than nano- or picoplankton (Table 3, Fig. 12d-f). Loss rates of pigments, estimated as the ratio of $P_{Pigment}$ fluxes to pigment standing stock, averaged (for all cruises) $8 \pm 12\%$ for microplankton pigments, $1 \pm 2\%$ for nanoplankton pigments and $0.6 \pm 1\%$ for picoplankton pigments. These results suggest that export of large cells by direct sinking of algal aggregates is more efficient than the export of small cells by the same pathway. Sediment trap loss rates for microplankton were also higher than those for nano- and picoplankton, further indicating preferential export of microplankton. Even though differences between bottle and pump samples may exaggerate the extent to which

435 large cells dominate export, sediment trap loss rates support and confirm the preferential export
436 of large cells by algal aggregation.

437 In contrast to the trends observed for pigment fluxes and loss rates, the low variability of
438 pump indicator pigment PFs with depth (Figs. 6-8) does not appear to indicate preferential export
439 of microplankton. Furthermore, the presence of nano- and picoplankton pigments in the >53- μ m
440 size-fraction and in samples below the mixed layer suggests that nano- and picoplankton are
441 incorporated into aggregates and that some of these aggregates are exported from the surface
442 ocean. If large cells were being preferentially exported, microplankton pigments would be
443 expected to make up a larger percentage of total pigments in samples below the mixed layer than
444 in samples from the mixed layer, but this is not observed in the results of this study. It is
445 possible that some of this discrepancy can be attributed to differences between bottle and pump
446 samples. Because cells <1- μ m in size can pass through the 1- μ m Nitex screens used in the
447 pumps, the sum of the pump size-fractions does not accurately reflect the community
448 composition in the euphotic zone, and may miss a change in indicator pigment PFs with depth.
449 In addition, the under-sampling of large cells by Niskin bottles may lead to an underestimate of
450 microplankton standing stocks, and thus and overestimate of microplankton loss rates.

451 These pigment fluxes are likely lower estimates of the total contribution of each
452 phytoplankton group to particle export. The use of indicator pigments as tracers of
453 phytoplankton export only accounts for the direct sinking of healthy, ungrazed cells, because
454 grazing degrades the indicator pigments to an analytically undetectable form (Head and Harris,
455 1992; Strom et al., 1998; Thibault et al., 1999). Indirect export (via grazing) is thought to be an
456 important pathway for picoplankton export in the HNLC Equatorial Pacific (Richardson et al.,
457 2004; Stukel and Landry, 2010). Given that grazing has been shown to control the biomass of
458 small phytoplankton in the northeast Pacific (Landry et al., 1993; Harrison et al., 1999; Rivkin et
459 al., 1999), indirect export may also be a significant pathway for small cell export in this region.
460 Because this pathway is not accounted for by the methodology employed in this study, the results
461 presented here may underestimate the export of small phytoplankton, which may be less likely to
462 sink directly.

463 Although grazing and fecal pellet export were not directly measured in this study, a
464 comparison of sediment trap and pump measurements of Chl *a*, indicator pigments, and POC,
465 suggests that zooplankton fecal pellets may be an important component of POC export at OSP, at

least in spring (Fig. 11). While F_{POC} fluxes are higher than the corresponding P_{POC} fluxes, $F_{Pigment}$ fluxes are lower than $P_{Pigment}$ fluxes, indicating that the material captured by the sediment traps is enriched in carbon and depleted in Chl *a* and indicator pigments relative to that sampled by the pumps. Because the trap brine was not poisoned, zooplankton grazing and cell degradation in the trap tube may also have contributed to some loss of pigments over the ~3 day deployment of the PITS traps. However, the collection of carbon-rich and pigment-depleted fecal pellets by the traps but not by the pumps, which do not quantitatively sample fecal pellets (Lomas and Moran, 2011), could also explain these observations. This latter explanation is consistent with the results presented in Thibault et al. (1999), which indicate that fecal pellet export is 3 to 6 times greater than algal aggregate export at Line P.

5 Conclusions

New estimates of phytoplankton indicator pigment loss rates calculated from both ^{234}Th -derived and sediment trap pigment fluxes suggest that large cells are preferentially exported at Line P. Specifically, microplankton pigments on average made up $69 \pm 19\%$ of the total pigment flux, but only $32 \pm 24\%$ of pigment standing stock (determined from small-volume samples), whereas nano- and picoplankton pigments on average formed $31 \pm 19\%$ of pigment flux in spite of representing $68 \pm 24\%$ of the standing stock. These results are consistent with traditional food web models (Michaels and Silver, 1988; Legendre and Le Fèvre, 1995) that suggest nano- and picoplankton are underrepresented in particle flux relative to their contribution to phytoplankton biomass; they also lend support to the conclusions of Choi et al. (2014). However, the methods employed in this study do not quantitatively account for export via zooplankton fecal pellets, which could be significant for small phytoplankton as they are controlled by grazing in this region (Landry et al., 1993; Harrison et al., 1999; Rivkin et al., 1999; Thibault et al., 1999). Furthermore, the determination of pigment loss rates also required a comparison between small- and large-volume samples, and the inherent differences of these sampling techniques likely led to an overestimation of the microplankton contribution to algal aggregate export. Therefore, it is possible that all sizes-classes of phytoplankton contribute to POC export in approximate proportion to their contribution to NPP as predicted by Richardson and Jackson (2007).

This study, conducted in a subarctic HNLC region, contributes to the ongoing discussion of small cell export that has largely focused on tropical and subtropical regions (Richardson et

al., 2004; Richardson et al., 2006; Richardson and Jackson, 2007; Stukel and Landry, 2010; Lomas and Moran, 2011). In particular, these results suggest that nano- and picoplankton may contribute significantly to POC export in this subarctic HNLC region, even if they are not as efficiently exported as larger microplankton. If large phytoplankton drive more efficient POC export in the northeast Pacific as suggested by this study, it could have important implications for understanding the biological pump. It has been proposed that decreasing winter mixed layer depths (Freeland et al., 1997; Freeland, 2013) and variations of macronutrient concentrations linked to shifts in climate regime (Pena and Varela, 2007) in the northeast Pacific could lead to shifts in the phytoplankton community composition. This study suggests that such changes in phytoplankton community composition could significantly affect the efficiency of the biological pump, and in turn, the cycling of carbon. While the results indicate that shifts in community composition favoring larger phytoplankton could lead to more efficient particle export, they do not indicate that shifts favoring smaller phytoplankton would lead to a shutdown of POC export as suggested by some previous studies (e.g., Michaels and Silver, 1988), but merely that the export of POC could be less efficient.

Acknowledgements

We thank the captain and crew of the CCGS *John P. Tully*, Marie Robert and the Line P Program collaborators, Doug Bell for at-sea sampling and laboratory assistance, and Matthew Baumann for his laboratory assistance. This research was supported by the National Science Foundation grants OCE 0926311 to SBM, OCE 0927559 to MWL, and OCE 0926348 to GMS.

528 References

- 529 [Amacher, J., Neuer, S., Anderson, I. and Massana, R.: Molecular approach to determine](#)
530 [contributions of the protist community to particle flux, Deep-Sea Res. Part Oceanogr. Res. Pap.,](#)
531 [56\(12\), 2206–2215, doi:10.1016/j.dsr.2009.08.007, 2009.](#)
- 532 [Baumann, M. S., Moran, S. B., Lomas, M. W., Kelly, R. P. and Bell, D. W.: Seasonal decoupling](#)
533 [of particulate organic carbon export and net primary production in relation to sea-ice at the shelf](#)
534 [break of the eastern Bering Sea: Implications for off-shelf carbon export, J. Geophys. Res.](#)
535 [Oceans, 118\(10\), 5504–5522, doi:10.1002/jgrc.20366, 2013.](#)
- 536 [Benitez-Nelson, C. R., Buesseler, K. O., Van der Loeff, M. R., Andrews, J., Ball, L., Crossin, G.](#)
537 [and Charette, M. A.: Testing a new small-volume technique for determining \$^{234}\text{Th}\$ in seawater,](#)
538 [J. Radioanal. Nucl. Chem., 248\(3\), 795–799, 2001.](#)
- 539 [Bograd, S. J., Thomson, R. E., Rabinovich, A. B. and LeBlond, P. H.: Near-surface circulation of](#)
540 [the northeast Pacific Ocean derived from WOCE-SVP satellite-tracked drifters, Deep Sea Res.](#)
541 [Part II Top. Stud. Oceanogr., 46\(11–12\), 2371 – 2403, doi:http://dx.doi.org/10.1016/S0967-](#)
542 [0645\(99\)00068-5, 1999.](#)
- 543 [Boyd, P. and Harrison, P. J.: Phytoplankton dynamics in the {NE} subarctic Pacific, Deep Sea](#)
544 [Res. Part II Top. Stud. Oceanogr., 46\(11–12\), 2405 – 2432, doi:http://dx.doi.org/10.1016/S0967-](#)
545 [0645\(99\)00069-7, 1999.](#)
- 546 [Boyd, P. W. and Newton, P. P.: Does planktonic community structure determine downward](#)
547 [particulate organic carbon flux in different oceanic provinces?, Deep Sea Res. Part Oceanogr.](#)
548 [Res. Pap., 46\(1\), 63 – 91, doi:http://dx.doi.org/10.1016/S0967-0637\(98\)00066-1, 1999.](#)
- 549 [Brew, H. S., Moran, S. B., Lomas, M. W. and Burd, A. B.: Plankton community composition,](#)
550 [organic carbon and thorium-234 particle size distributions, and particle export in the Sargasso](#)
551 [Sea, J. Mar. Res., 67\(6\), 845–868, doi:10.1357/002224009792006124, 2009.](#)
- 552 [Buesseler, K. O.: The decoupling of production and particulate export in the surface ocean, Glob.](#)
553 [Biogeochem. Cycles, 12\(2\), 297–310, doi:10.1029/97GB03366, 1998.](#)
- 554 [Buesseler, K. O., Benitez-Nelson, C., Rutgers van der Loeff, M., Andrews, J., Ball, L., Crossin,](#)
555 [G. and Charette, M. A.: An intercomparison of small-and large-volume techniques for thorium-](#)
556 [234 in seawater, Mar. Chem., 74\(1\), 15–28, 2001.](#)
- 557 [Burd, A. B., Jackson, G. A. and Moran, S. B.: The role of the particle size spectrum in estimating](#)
558 [POC fluxes from disequilibrium, Deep Sea Res. Part Oceanogr. Res. Pap., 54\(6\), 897–918, 2007.](#)
- 559 [Charette, M. A., Moran, S. B. and Bishop, J. K. B.: \$^{234}\text{Th}\$ as a tracer of particulate organic carbon](#)
560 [export in the subarctic northeast Pacific Ocean, Deep Sea Res. Part II Top. Stud. Oceanogr.,](#)
561 [46\(11–12\), 2833 – 2861, doi:http://dx.doi.org/10.1016/S0967-0645\(99\)00085-5, 1999.](#)
- 562 [Chen, J. H., Lawrence Edwards, R. and Wasserburg, G. J.: \$^{238}\text{U}\$, \$^{234}\text{U}\$ and \$^{232}\text{Th}\$ in seawater,](#)
563 [Earth Planet. Sci. Lett., 80\(3\), 241–251, 1986.](#)

564 [Choi, H. Y., Stewart, G. M., Lomas, M. W., Kelly, R. P. and Moran, S. B.: Linking the](#)
565 [distribution of ²¹⁰Po and ²¹⁰Pb with plankton community along Line P, Northeast Subarctic](#)
566 [Pacific, J. Environ. Radioact., 2014.](#)

567 [Coale, K. H. and Bruland, K. W.: ²³⁴Th: ²³⁸U disequilibria within the California Current,](#)
568 [Limnol Ocean., 30\(1\), 22–33, 1985.](#)

569 [Emerson, S.: Annual net community production and the biological carbon flux in the ocean,](#)
570 [Glob. Biogeochem. Cycles, 2014.](#)

571 [Freeland, H., Denman, K., Wong, C. S., Whitney, F. and Jacques, R.: Evidence of change in the](#)
572 [winter mixed layer in the Northeast Pacific Ocean, Deep Sea Res. Part Oceanogr. Res. Pap.,](#)
573 [44\(12\), 2117 – 2129, doi:http://dx.doi.org/10.1016/S0967-0637\(97\)00083-6, 1997.](#)

574 [Freeland, H. J.: Evidence of Change in the Winter Mixed Layer in the Northeast Pacific Ocean:](#)
575 [A Problem Revisited, Atmosphere-Ocean, 51\(1\), 126–133, 2013.](#)

576 [Gardner, W. D.: Incomplete extraction of rapidly settling particles from water samplers, Limnol](#)
577 [Ocean., 22\(4\), 764–768, 1977.](#)

578 [Gundersen, K., Orcutt, K. M., Purdie, D. A., Michaels, A. F. and Knap, A. H.: Particulate](#)
579 [organic carbon mass distribution at the Bermuda Atlantic Time-series Study \(BATS\) site, Deep](#)
580 [Sea Res. Part II Top. Stud. Oceanogr., 48\(8\), 1697–1718, 2001.](#)

581 [Harrison, P. J.: SERIES \(subarctic ecosystem response to iron enrichment study\): A Canadian–](#)
582 [Japanese contribution to our understanding of the iron–ocean–climate connection, Deep Sea Res.](#)
583 [Part II Top. Stud. Oceanogr., 53\(20\), 2006.](#)

584 [Harrison, P. J., Boyda, P. W., Varela, D. E., Takeda, S., Shiimoto, A. and Odate, T.:](#)
585 [Comparison of factors controlling phytoplankton productivity in the {NE} and {NW} subarctic](#)
586 [Pacific gyres, Prog. Oceanogr., 43\(2–4\), 205 – 234, doi:http://dx.doi.org/10.1016/S0079-](#)
587 [6611\(99\)00015-4, 1999.](#)

588 [Head, E. J. H. and Harris, L. R.: Chlorophyll and carotenoid transformation and destruction by](#)
589 [Calanus spp. grazing on diatoms, Mar. Ecol.-Prog. Ser., 86, 229–229, 1992.](#)

590 [Hooker, S. B., Van Heukelem, L., Thomas, C. S., Claustre, H., Ras, J., Barlow, R., Sessions, H.,](#)
591 [Schlüter, L., Perl, J. and Trees, C.: Second SeaWiFS HPLC Analysis Round-robin Experiment](#)
592 [\(SeaHARRE-2\), National Aeronautics and Space Administration, Goddard Space Flight Center.,](#)
593 [2005.](#)

594 [Irwin, A. J., Finkel, Z. V., Schofield, O. M. E. and Falkowski, P. G.: Scaling-up from nutrient](#)
595 [physiology to the size-structure of phytoplankton communities, J. Plankton Res., 28\(5\), 459–471,](#)
596 [doi:10.1093/plankt/fbi148, 2006.](#)

597 [Knap, A. H., Michaels, A. F., Steinberg, D. K., Bahr, F., Bates, N. R., Bell, S., Countway, P.,](#)
598 [Close, A. R., Doyle, A. P. and Dow, R. L.: BATS Methods manual, version 4., 1997.](#)

Landry, M. R., Monger, B. C. and Selph, K. E.: Time-dependency of microzooplankton grazing and phytoplankton growth in the subarctic Pacific, *Prog. Oceanogr.*, 32(1–4), 205 – 222, doi:[http://dx.doi.org/10.1016/0079-6611\(93\)90014-5](http://dx.doi.org/10.1016/0079-6611(93)90014-5), 1993.

Legendre, L. and Le Fèvre, J.: Microbial food webs and the export of biogenic carbon in oceans, *Aquat. Microb. Ecol.*, 9(1), 69–77, 1995.

Liu, Z., Cochran, J. K., Lee, C., Gasser, B., Miquel, J. C. and Wakeham, S. G.: Further investigations on why {POC} concentrations differ in samples collected by Niskin bottle and in situ pump, *Deep Sea Res. Part II Top. Stud. Oceanogr.*, 56(18), 1558 – 1567, doi:<http://dx.doi.org/10.1016/j.dsr2.2008.12.019>, 2009.

Liu, Z., Stewart, G., Kirk Cochran, J., Lee, C., Armstrong, R. A., Hirschberg, D. J., Gasser, B. and Miquel, J.-C.: Why do POC concentrations measured using Niskin bottle collections sometimes differ from those using in-situ pumps?, *Deep Sea Res. Part Oceanogr. Res. Pap.*, 52(7), 1324–1344, doi:[10.1016/j.dsr.2005.02.005](http://dx.doi.org/10.1016/j.dsr.2005.02.005), 2005.

Van der Loeff, M. R., Sarin, M. M., Baskaran, M., Benitez-Nelson, C., Buesseler, K. O., Charette, M., Dai, M., Gustafsson, Ö., Masque, P. and Morris, P. J.: A review of present techniques and methodological advances in analyzing ^{234}Th in aquatic systems, *Mar. Chem.*, 100(3), 190–212, 2006.

Lomas, M. W. and Moran, S. B.: Evidence for aggregation and export of cyanobacteria and nano-eukaryotes from the Sargasso Sea euphotic zone, *Biogeosciences*, 8(1), 203–216, doi:[10.5194/bg-8-203-2011](http://dx.doi.org/10.5194/bg-8-203-2011), 2011.

Lomas, M. W., Moran, S. B., Casey, J. R., Bell, D. W., Tiahlo, M., Whitefield, J., Kelly, R. P., Mathis, J. T. and Coklet, E. D.: Spatial and seasonal variability of primary production on the Eastern Bering Sea shelf, *Deep Sea Res. Part II Top. Stud. Oceanogr.*, 65–70(0), 126 – 140, doi:<http://dx.doi.org/10.1016/j.dsr2.2012.02.010>, 2012.

Marchetti, A., Sherry, N. D., Kiyosawa, H., Tsuda, A. and Harrison, P. J.: Phytoplankton processes during a mesoscale iron enrichment in the NE subarctic Pacific: Part I—biomass and assemblage, *Deep Sea Res. Part II Top. Stud. Oceanogr.*, 53(20), 2095–2113, 2006.

McNally, G. J.: Satellite - tracked drift buoy observations of the near - surface flow in the eastern mid - latitude North Pacific, *J. Geophys. Res. Oceans* 1978–2012, 86(C9), 8022–8030, 1981.

Michaels, A. F. and Silver, M. W.: Primary production, sinking fluxes and the microbial food web, *Deep Sea Res. Part Oceanogr. Res. Pap.*, 35(4), 473 – 490, doi:[http://dx.doi.org/10.1016/0198-0149\(88\)90126-4](http://dx.doi.org/10.1016/0198-0149(88)90126-4), 1988.

Moran, S. B., Charette, M. A., Pike, S. M. and Wicklund, C. A.: Differences in seawater particulate organic carbon concentration in samples collected using small-and large-volume methods: the importance of DOC adsorption to the filter blank, *Mar. Chem.*, 67(1), 33–42, 1999.

635 [Moran, S. B., Weinstein, S. E., Edmonds, H. N., Smith, J. N., Kelly, R. P., Pilson, M. E. Q. and](#)
 636 [Harrison, W. G.: Does \$^{234}\text{Th}/^{238}\text{U}\$ disequilibrium provide an accurate record of the export flux](#)
 637 [of particulate organic carbon from the upper ocean?, *Limnol. Oceanogr.*, 48\(3\), 1018–1029,](#)
 638 [2003.](#)

639 [Morán, X. A. G., López-Urrutia, Á., Calvo - Díaz, A. and Li, W. K.: Increasing importance of](#)
 640 [small phytoplankton in a warmer ocean, *Glob. Change Biol.*, 16\(3\), 1137–1144, 2010.](#)

641 [Muggli, D. L., Lecourt, M. and Harrison, P. J.: Effects of iron and nitrogen source on the sinking](#)
 642 [rate, physiology and metal composition of an oceanic diatom from the subarctic Pacific,](#)
 643 [Oceanogr. Lit. Rev., 43\(11\), 1996.](#)

644 [Pena, M. A. and Varela, D. E.: Seasonal and interannual variability in phytoplankton and nutrient](#)
 645 [dynamics along Line P in the NE subarctic Pacific, *Prog. Oceanogr.*, 75\(2\), 200–222, 2007.](#)

646 [Polovina, J. J., Howell, E. A. and Abecassis, M.: Ocean's least productive waters are expanding,](#)
 647 [Geophys. Res. Lett., 35\(3\), 2008.](#)

648 [Richardson, T. L. and Jackson, G. A.: Small phytoplankton and carbon export from the surface](#)
 649 [ocean, *Science*, 315\(5813\), 838–840, 2007.](#)

650 [Richardson, T. L., Jackson, G. A., Ducklow, H. W. and Roman, M. R.: Carbon fluxes through](#)
 651 [food webs of the eastern equatorial Pacific: an inverse approach, *Deep Sea Res. Part Oceanogr.*](#)
 652 [Res. Pap., 51\(9\), 1245–1274, doi:10.1016/j.dsr.2004.05.005, 2004.](#)

653 [Richardson, T. L., Jackson, G. A., Ducklow, H. W. and Roman, M. R.: Spatial and seasonal](#)
 654 [patterns of carbon cycling through planktonic food webs of the Arabian Sea determined by](#)
 655 [inverse analysis, *US JGOFS Synth. Model. Proj. Phase III US JGOFS Synth. Model. Proj. Phase*](#)
 656 [III, 53\(5–7\), 555–575, doi:10.1016/j.dsr2.2006.01.015, 2006.](#)

657 [Rivkin, R. B., Putland, J. N., Robin Anderson, M. and Deibel, D.: Microzooplankton bacterivory](#)
 658 [and herbivory in the NE subarctic Pacific, *Deep Sea Res. Part II Top. Stud. Oceanogr.*, 46\(11\),](#)
 659 [2579–2618, 1999.](#)

660 [Speicher, E. A., Moran, S. B., Burd, A. B., Delfanti, R., Kaberi, H., Kelly, R. P., Papucci, C.,](#)
 661 [Smith, J. N., Stavrakakis, S. and Torricelli, L.: Particulate organic carbon export fluxes and size-](#)
 662 [fractionated POC/ \$^{234}\text{Th}\$ ratios in the Ligurian, Tyrrhenian and Aegean Seas, *Deep Sea Res. Part*](#)
 663 [Oceanogr. Res. Pap., 53\(11\), 1810–1830, 2006.](#)

664 [Strom, S., Morello, T. and Bright, K.: Protozoan size influences algal pigment degradation](#)
 665 [during grazing, *Mar. Ecol. Prog. Ser. Halstenbek*, 164, 189–197, doi:10.3354/meps164189,](#)
 666 [1998.](#)

667 [Stukel, M. R., Décima, M., Selph, K. E., Taniguchi, D. A. and Landry, M. R.: The role of](#)
 668 [Synechococcus in vertical flux in the Costa Rica upwelling dome, *Prog. Oceanogr.*, 112, 49–59,](#)
 669 [2013.](#)

670 [Stukel, M. R. and Landry, M. R.: Contribution of picophytoplankton to carbon export in the](#)
671 [equatorial Pacific: A reassessment of food web flux inferences from inverse models, *Limnol.*](#)
672 [Oceanogr., 55\(6\), 2669–2685, 2010.](#)

673 [Thibault, D., Roy, S., Wong, C. S. and Bishop, J. K.: The downward flux of biogenic material in](#)
674 [the NE subarctic Pacific: importance of algal sinking and mesozooplankton herbivory, *Deep Sea*](#)
675 [Res. Part II Top. Stud. Oceanogr., 46\(11\), 2669–2697, 1999.](#)

676 [Timothy, D. A., Wong, C. S., Barwell-Clarke, J. E., Page, J. S., White, L. A. and Macdonald, R.](#)
677 [W.: Climatology of sediment flux and composition in the subarctic Northeast Pacific Ocean with](#)
678 [biogeochemical implications, *Prog. Oceanogr.*, 116, 95–129, 2013.](#)

679 [Wong, C. S., Whitney, F. A., Crawford, D. W., Iseki, K., Matear, R. J., Johnson, W. K., Page, J.](#)
680 [S. and Timothy, D.: Seasonal and interannual variability in particle fluxes of carbon, nitrogen](#)
681 [and silicon from time series of sediment traps at Ocean Station P, 1982–1993: Relationship to](#)
682 [changes in subarctic primary productivity, *Deep Sea Res. Part II Top. Stud. Oceanogr.*, 46\(11\),](#)
683 [2735–2760, 1999.](#)

684
685
686
687
688
689
690
691
692
693
694
695
696
697
698
699
700

Table 1: Cruise dates and sample collection along Line P

Cruise Dates	P4	P12	P16	P20	P26
2010-14	Total Th	Total Th	Total Th	Total Th	Total Th

701
702
703
704
705
706
707
708
709
710
711

<u>Aug. 2010</u>	-	-	-	-	-
<u>(8/19/10 - 8/31/10)</u>	-	<u>WC Pig</u>	<u>WC Pig</u>	<u>WC Pig</u>	-
<u>2011-01</u>	-	<u>Total Th</u>	<u>Total Th</u>	<u>Total Th</u>	<u>Total Th</u>
<u>Feb. 2011</u>	-	-	-	-	-
<u>(2/9/11 - 2/15/11)</u>	-	<u>WC Pig</u>	<u>WC Pig</u>	<u>WC Pig</u>	-
<u>2011-26</u>	<u>Total Th</u>	<u>Total Th</u>	<u>Total Th</u>	<u>Total Th</u>	<u>Total Th</u>
<u>June 2011</u>	-	-	-	-	<u>Part. Th</u>
<u>(6/4/11 - 6/16/11)</u>	<u>WC Pig</u>	<u>WC Pig</u>	<u>WC Pig</u>	<u>WC Pig</u>	<u>WC Pig</u>
-	-	-	-	-	<u>Part. Pig</u>
-	-	-	-	-	<u>Traps</u>
<u>2012-01</u>	<u>Total Th</u>	<u>Total Th</u>	<u>Total Th</u>	<u>Total Th</u>	<u>Total Th</u>
<u>Feb. 2012</u>	<u>Part. Th</u>	<u>Part. Th</u>	-	-	<u>Part. Th</u>
<u>(2/7/12 - 2/19/12)</u>	<u>WC Pig</u>	<u>WC Pig</u>	-	-	<u>WC Pig</u>
-	<u>Part. Pig</u>	<u>Part. Pig</u>	-	-	<u>Part. Pig</u>
<u>2012-12</u>	<u>Total Th</u>	<u>Total Th</u>	<u>Total Th</u>	<u>Total Th</u>	<u>Total Th</u>
<u>June 2012</u>	<u>Part. Th</u>	<u>Part. Th</u>	<u>Part. Th</u>	<u>Part. Th</u>	<u>Part. Th</u>
<u>(5/23/12 - 6/7/12)</u>	<u>WC Pig</u>	<u>WC Pig</u>	<u>WC Pig</u>	-	-
-	<u>Part. Pig</u>	<u>Part. Pig</u>	<u>Part. Pig</u>	<u>Part. Pig</u>	<u>Part. Pig</u>
-	-	-	-	-	<u>Traps</u>

Table 2: Total net primary production (NPP) and >5 μm size-fractionated NPP determined from simulated in situ incubations.
²³⁴Th-derived POC flux (P_{POC}) and sediment trap POC flux (Trap_{POC}) determined at the base of the photic zone and the corresponding *ThE*-ratios ($P_{\text{POC}}/\text{NPP}$) and trap *e*-ratios ($\text{Trap}_{\text{POC}}/\text{NPP}$).

<u>Cruise</u>	<u>Station</u>	<u>Integration Depth (m)</u>	<u>Total NPP (mmol m⁻² d⁻¹)</u>	<u>>5 µm NPP (mmol m⁻² d⁻¹)</u>	<u>P_{POC} (mmol m⁻² d⁻¹)</u>	<u>Trap_{POC} (mmol m⁻² d⁻¹)</u>	<u>ThE-ratio</u>	<u>Trap e-ratio</u>
<u>Feb. 2011</u>	<u>P20</u>	<u>77</u>	<u>36.64</u>	<u>3.26</u>				
<u>June 2011</u>	<u>P26-D</u>	<u>83</u>	<u>105.14</u>	<u>13.67</u>	<u>2.94</u>	<u>5.91</u>	<u>0.03</u>	<u>0.06</u>
	<u>P26-R</u>	<u>85</u>	<u>78.75</u>	<u>12.98</u>	<u>2.75</u>	<u>5.91</u>	<u>0.03</u>	<u>0.08</u>
<u>Feb. 2012</u>	<u>P4</u>	<u>50</u>	<u>27.91</u>	<u>3.58</u>	<u>7.29</u>		<u>0.26</u>	
	<u>P12</u>	<u>95</u>	<u>34.56</u>	<u>4.58</u>	<u>4.65</u>		<u>0.13</u>	
	<u>P26</u>	<u>75</u>	<u>23.41</u>	<u>5.22</u>	<u>0.31</u>		<u>0.01</u>	
<u>June 2012</u>	<u>P4</u>	<u>103</u>	<u>82.36</u>	<u>39.55</u>	<u>7.95</u>		<u>0.10</u>	
	<u>P12</u>	<u>164</u>	<u>40.24</u>	<u>4.16</u>	<u>2.12</u>		<u>0.05</u>	
	<u>P20</u>	<u>115</u>	<u>57.84</u>	<u>4.10</u>	<u>0.54</u>		<u>0.01</u>	
<u>-</u>	<u>P26</u>	<u>60</u>	<u>49.45</u>	<u>9.28</u>	<u>2.96</u>	<u>6.55</u>	<u>0.06</u>	<u>0.13</u>

712
713
714
715
716
717
718
719
720
721
722
723
724

Table 3: Chl *a* and indicator pigment standing stocks determined by integrating small volume pigment concentrations (determined by HPLC) across the photic zone, pigment fluxes (^{234}Th and PITS-derived) measured at the base of the photic zone, and pigment loss rates, or the percent of the surface concentration represented by those fluxes. Pigment standing stocks are in mg m^{-2} and pigment fluxes are in $\text{mg m}^{-2} \text{d}^{-1}$.

Cruise	Station	Depth	Chl <i>a</i>	FUCO	PER	HEX	BUT	ALLO	Chl <i>b</i>	ZEA
Aug. 2010 (2010-14)	P12	Surface (1-75 m)	23.918	3.498	0.375	7.705	1.165	0.220	4.038	1.435
	P16	Surface (1-75 m)	14.165	1.288	0.340	6.010	1.018	0.065	2.588	0.165
	P20	Surface (1-75 m)	19.040	3.138	0.398	6.298	1.453	0.065	2.620	0.188
Feb. 2011 (2011-01)	P12	Surface (1-65 m)	30.122	2.848	0.379	5.630	2.431	0.838	7.133	0.922
	P16	Surface (1-95 m)	16.230	1.286	0.202	5.728	1.726	0.161	4.439	1.643
	P20	Surface (1-77 m)	55.053	5.207	0.689	18.064	6.697	1.116	11.435	4.516
June 2011 (2011-26)	P4	Surface (1-72 m)	29.791	2.635	0.127	10.619	2.663	0.720	5.836	5.234
	P12	Surface (1-90 m)	26.115	5.060	0.085	11.988	3.263	0.498	2.665	3.063
	P16	Surface (1-105 m)	22.088	4.044	0.104	11.390	2.195	0.181	2.612	1.569
	P20	Surface (1-70 m)	19.421	4.423	0.197	8.132	1.913	0.166	2.090	1.129
	P26	Surface (1-84 m)	29.376	7.239	0.184	10.532	4.406	0.232	3.723	2.663
		Flux at 100 m	0.765	0.474	0.036	0.059	0.0002	0.016	0.028	0.018
		% Flux	2.605	6.548	$\frac{19.76}{2}$	0.564	0.004	6.686	0.753	0.658
		Trap (150 m)	0.125	0.056	0.027	0.049	0.014	-	0.017	0.015
		% Flux	0.424	0.767	$\frac{14.87}{9}$	0.466	0.311	-	0.461	0.545

Feb. 2012 (2012-01)	P4	Surface (1-38 m)	22.684	3.765	-	4.592	1.434	0.917	3.781	0.280
		Flux at 50 m	3.283	1.863		0.811	0.122			
		% Flux	14.471	49.468	-	17.668	8.537	-	-	-
	P12	Surface (1-38 m)	11.003	1.425	0.116	5.606	1.894	0.017	1.915	0.500
		Flux at 100 m	0.046	0.020	0.000	0.014	0.005	0.000	0.000	0.000
		% Flux	0.415	1.381	0.000	0.254	0.249	0.000	0.000	0.000
	P26	Surface (1-38 m)	12.161	2.092	1.218	2.923	1.615	0.137	0.902	0.228
		Flux at 100 m	0.380	0.251	0.035	0.046	0.038	0.000	0.014	0.045
		% Flux	3.126	11.999	2.898	1.581	2.373	0.000	1.524	19.919
June 2012 (2012-12)	P4	Surface (1-103 m)	21.313	31.420	-	5.192	-	-	-	-
		Flux at 200 m	1.076	0.919	0.047	0.126	-	-	-	0.036
		% Flux	5.047	2.926	-	2.435	-	-	-	-
	P12	Surface (1-164 m)	27.677	5.967	-	22.445	6.552	-	-	-
		Flux at 200 m	0.051	0.047	-	0.075	0.010	-	0.025	-
		% Flux	0.185	0.787	-	0.335	0.156	-	-	-
	P16	Surface (1-66 m)	12.830	8.722	-	17.321	4.238	-	0.942	0.777
		Flux at 100 m	0.312	0.319	0.045	0.044	0.007	-	-	-
		% Flux	2.431	3.662	-	0.252	0.174	-	-	-
	P20	Surface (1-115 m)	18.344	33.038	-	13.892	-	-	13.090	3.538
		Flux at 100 m	0.016	0.016	0.004	-	0.002	-	0.005	0.001
		% Flux	0.088	0.049	-	-	-	-	0.036	0.033
	P26	Surface (1-60 m)	14.024	1.977	-	13.572	2.018	-	4.969	2.768
		Flux at 100 m	0.255	0.304	-	-	0.029	-	0.025	-
		% Flux	1.821	15.359	-	-	1.437	-	0.507	-
		Trap (100 m)	0.055	0.025	0.006	0.041	0.004	-	0.009	0.008
		% Flux	0.393	1.243	-	0.304	0.190	-	0.179	0.288

725

726

727

728

Table 4: ^{234}Th and POC fluxes and POC/ ^{234}Th ratios measured by the PITS traps.

Depth (m)	Days In-situ	^{234}Th flux (dpm m ⁻² d ⁻¹)	POC flux (mmol m ⁻² d ⁻¹)	POC/ ^{234}Th ratio ($\mu\text{mol dpm}^{-1}$)
June 2011 P26				
30	3.32	3192 ± 117	15.3 ± 0.4	4.8 ± 0.2
50	3.32	2909 ± 92	10.1 ± 0.3	3.5 ± 0.1
100	3.32	2256 ± 94	5.9 ± 0.2	2.6 ± 0.1
150	3.32	1928 ± 79	5.0 ± 0.2	2.6 ± 0.1
200	3.32	2281 ± 97	8.5 ± 0.3	3.7 ± 0.2
June 2012 P26				
30	2.82	3999 ± 206	14.7 ± 0.4	3.7 ± 0.2
50	2.82	5485 ± 290	13.5 ± 0.5	2.5 ± 0.2
100	2.82	3154 ± 192	6.5 ± 0.2	2.1 ± 0.1
150	2.82	2151 ± 135	5.5 ± 0.2	2.5 ± 0.2
200	2.82	3959 ± 129	5.0 ± 0.2	1.3 ± 0.1

729

730

731

732

733

734

735

736

737

738

739

740

741

742

743

744

745

746

747

748 Figure 1. Map showing the Line P stations sampled in this study.
749

750 Figure 2. Temperature ($^{\circ}\text{C}$), Sigma-t (kg m^{-3}), and $^{234}\text{Th}/^{238}\text{U}$ activity ratio distributions along
751 Line P cruises in August 2010, February 2011, June 2011, February 2012, and June 2012.
752

753 Figure 3. Comparison of small-volume Niskin bottle and large-volume in situ pump
754 measurements of a) POC, b) picoplankton indicator pigments, c) nanoplankton indicator
755 pigments, d) microplankton pigments. Niskin bottle measurements are lower than pump
756 measurements for microplankton pigments, and higher for nanoplankton pigments and POC.
757

758 Figure 4. a) $\text{POC}/^{234}\text{Th}$ ratios on 1 – 10- μm particles and on 10 – 53- μm particles plotted against
759 the $\text{POC}/^{234}\text{Th}$ ratio on >53- μm particles. Fractional distributions of POC and particulate ^{234}Th
760 are plotted for three size-classes of particles. The percentage of total POC associated with each
761 particle size-class is plotted against the percentage of total particulate ^{234}Th for samples collected
762 at stations on Line P during b) June 2011, c) February 2012, and d) June 2012. The correlation
763 coefficient (r^2) and the slope of the linear regression (m) are shown for each cruise.
764

765 Figure 5. Pigment Proportion Factors (PF) for each phytoplankton size-class plotted as a
766 function of sample depth at stations sampled on Line P during the five cruises in the study. All
767 data were collected from Niskin bottles.
768

769 Figure 6. Pigment PF for each phytoplankton size group plotted as a function of sample depth
770 and particle size-class at stations sampled on Line P in June 2011. Size-fractionated data are pump
771 data. Sediment trap PF's are also included.
772

773 Figure 7. Pigment PF for each phytoplankton size group plotted as a function of sample depth
774 and particle size-class at stations sampled on Line P in February 2012. Size-fractionated data are
775 pump data.
776

Figure 8. Pigment PF for each phytoplankton size group plotted as a function of sample depth and particle size-class at stations sampled on Line P in June 2012. Size-fractionated data are pump data. Sediment trap PF's are also included where available.

Figure 9. Depth profiles of a) ^{234}Th fluxes (P_{Th}) determined using the 2-D model, b) $\text{POC}/^{234}\text{Th}$ ratios on $>53\ \mu\text{m}$ particles, and c) ^{234}Th -derived POC fluxes (P_{POC}) at stations on Line P during the five cruises in this study.

Figure 10. Net primary production (NPP) plotted against ^{234}Th -derived POC fluxes (P_{POC}) for stations along Line P in this study. The slopes of the dashed lines represent ThE -ratios. For reference NPP and P_{POC} values determined by Charette et al. (1999) for winter, spring and summer are included, along with annual average NPP and sediment trap POC fluxes (at 200 m) reported in Harrison (2002) and Wong et al. (1999) respectively.

Figure 11. a) Comparison of sediment trap POC fluxes and ^{234}Th -derived POC fluxes, and b) a comparison of sediment trap Chl *a* and total indicator pigment fluxes and ^{234}Th -derived pigments fluxes at OSP during June 2011 and June 2012.

Figure 12. a-c) ^{234}Th -derived indicator pigment fluxes determined using the Pigment/ ^{234}Th ratio on $>53\text{-}\mu\text{m}$ particles plotted for micro-, nano-, and picoplankton pigments. d-f) Indicator pigment standing stocks plotted against indicator pigment fluxes for micro-, nano-, and picoplankton pigments. The slopes of the dashed lines indicate pigment loss rates. g-i) The contribution to total pigment standing stock plotted against the contribution to total pigment flux for micro-, nano-, and picoplankton pigments. Data points above the 1:1 line indicate preferential export by direct sinking and points below the 1:1 line indicate disproportionately low export by direct sinking relative to biomass contributions.

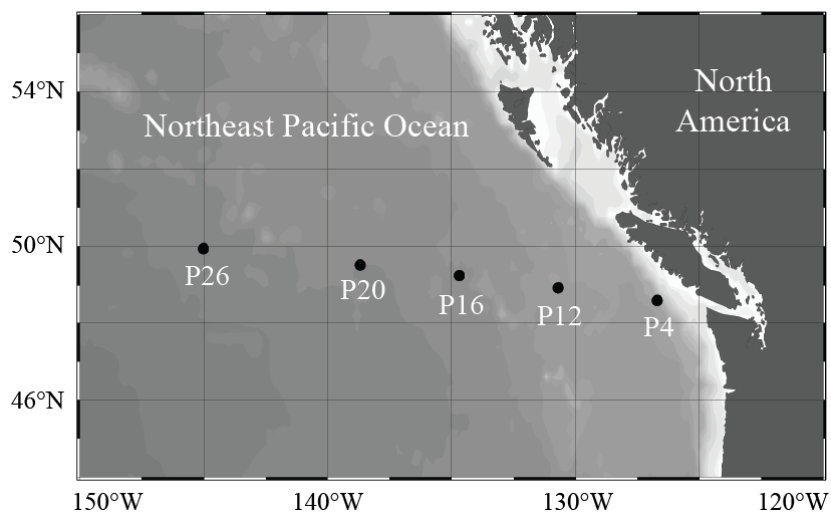


Fig. 1.

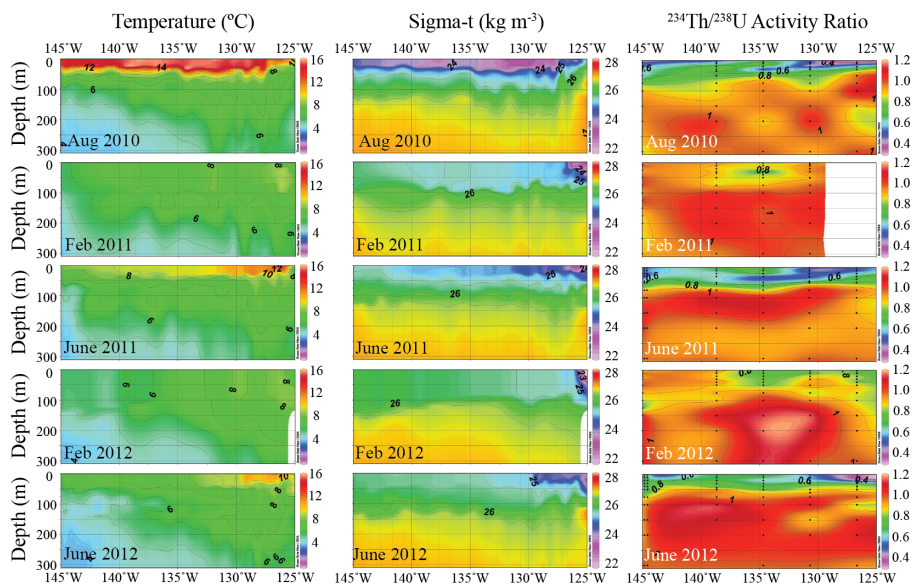


Fig. 2.

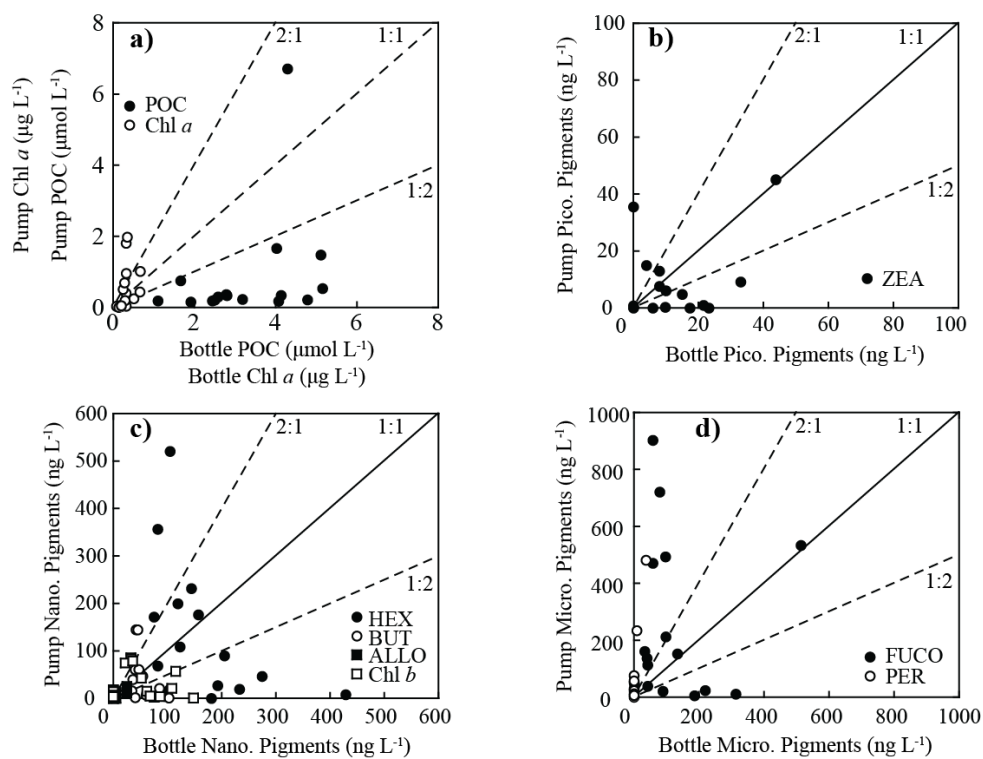


Fig. 3.

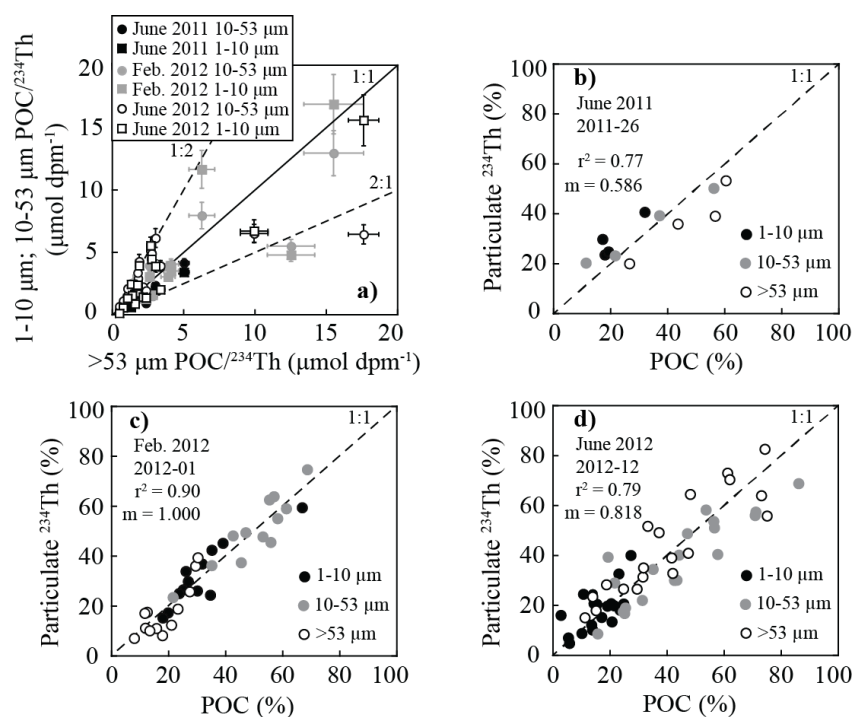


Fig. 4.

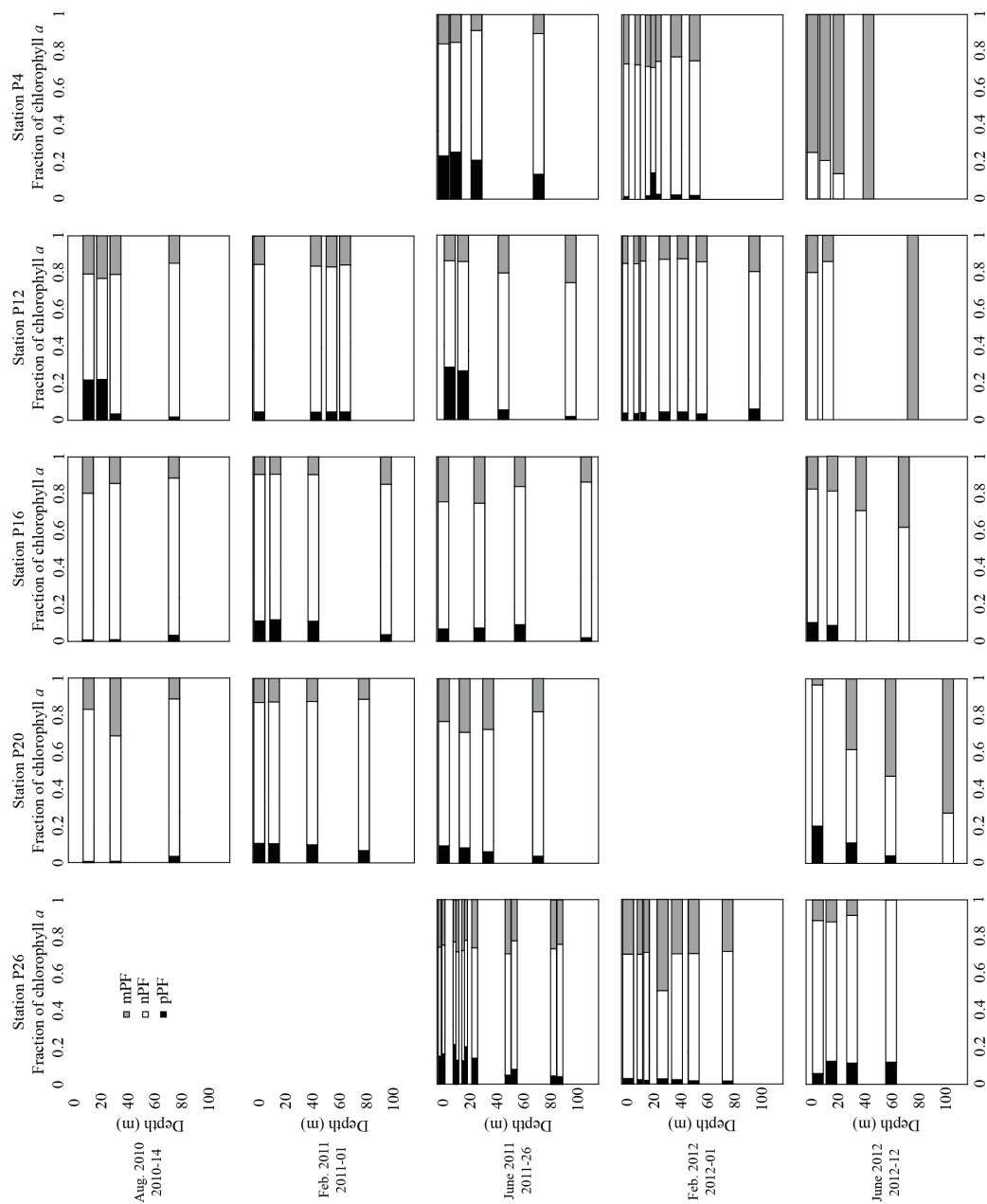
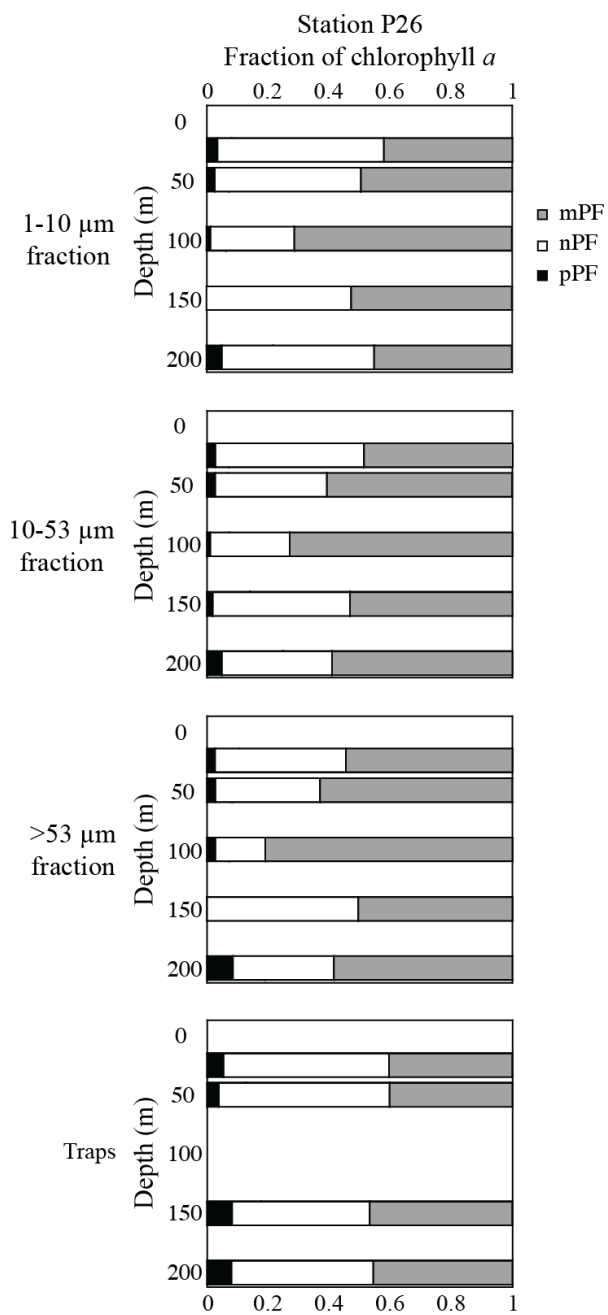


Fig. 5.



861 Fig. 6.
862

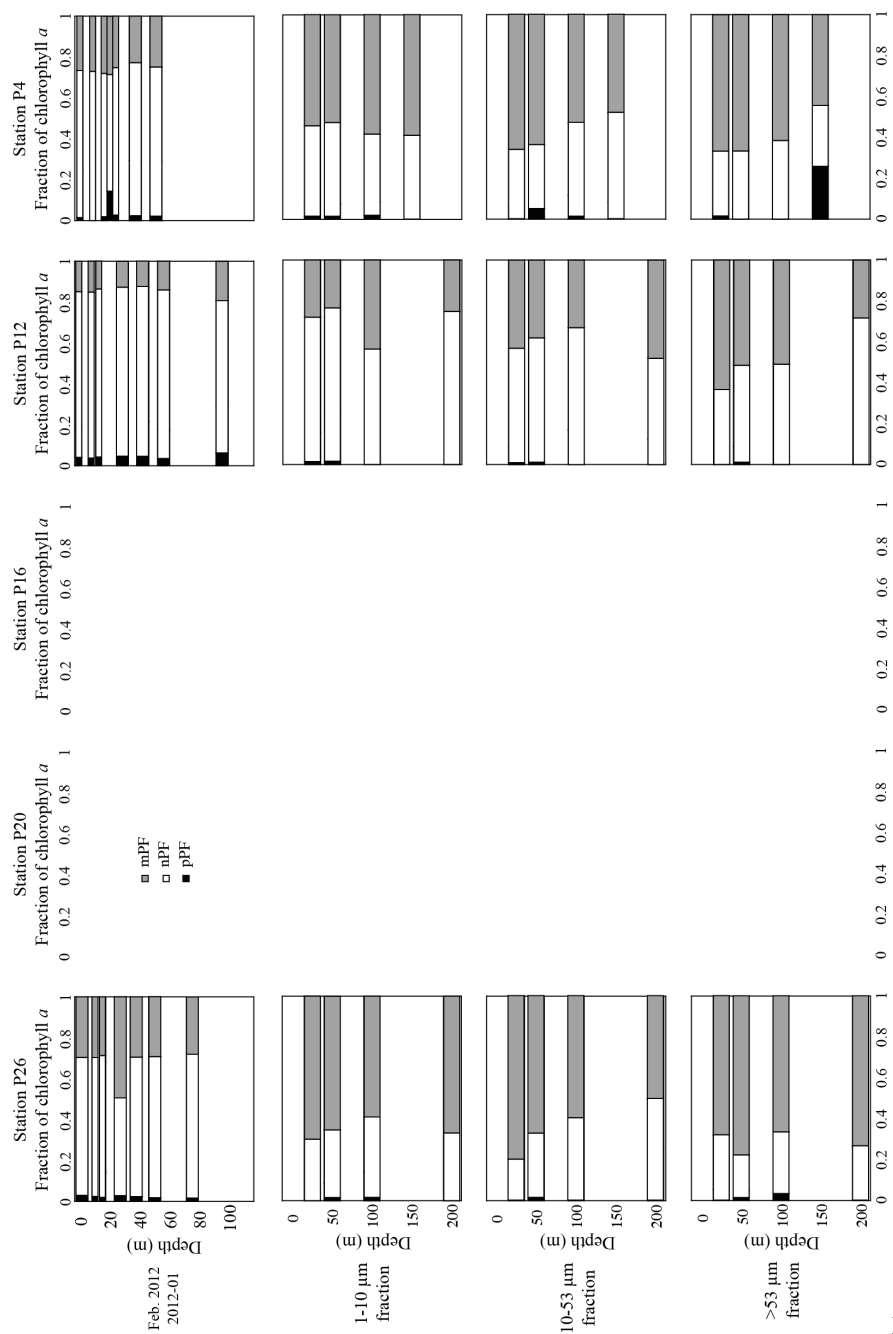


Fig. 7.

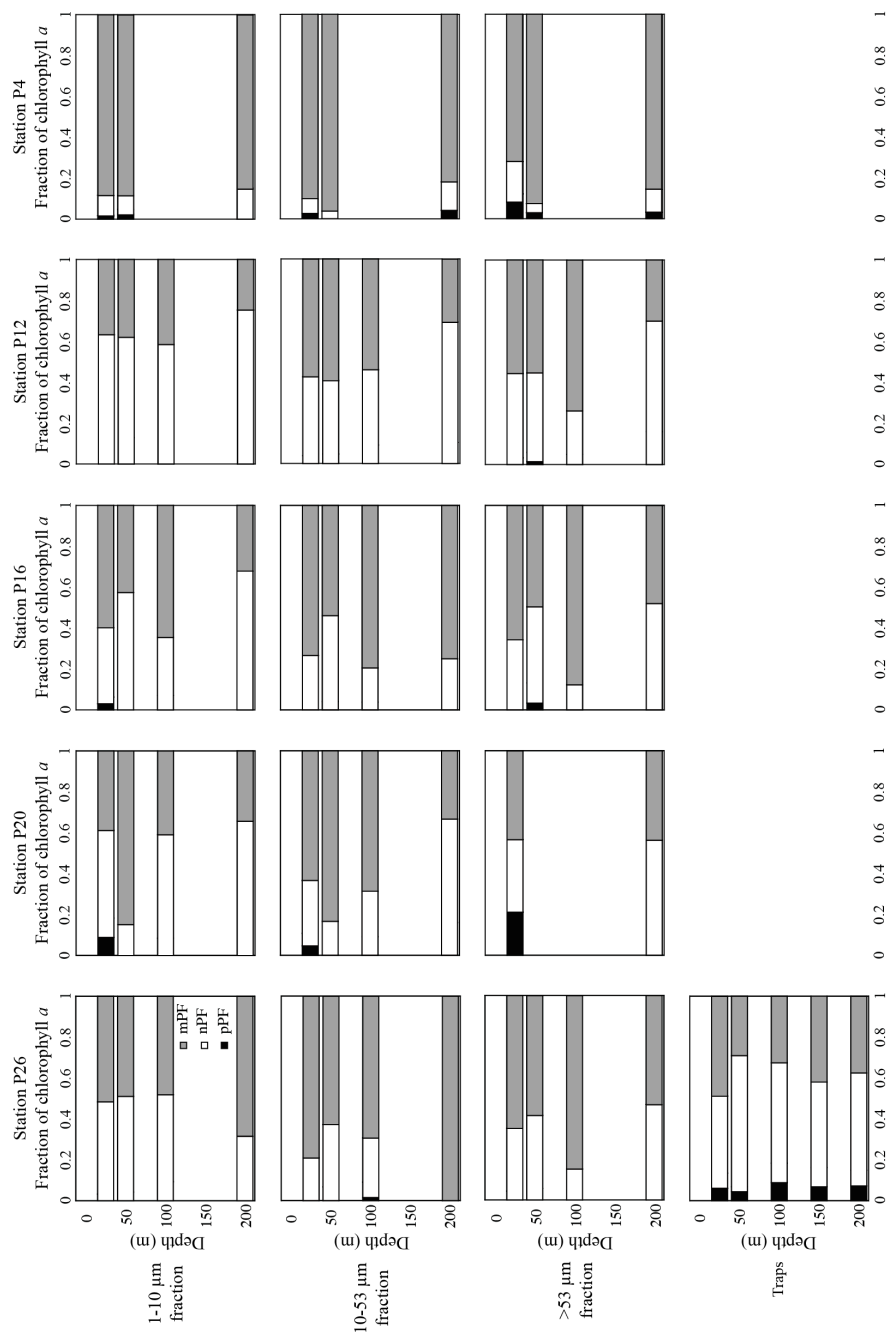


Fig. 8.

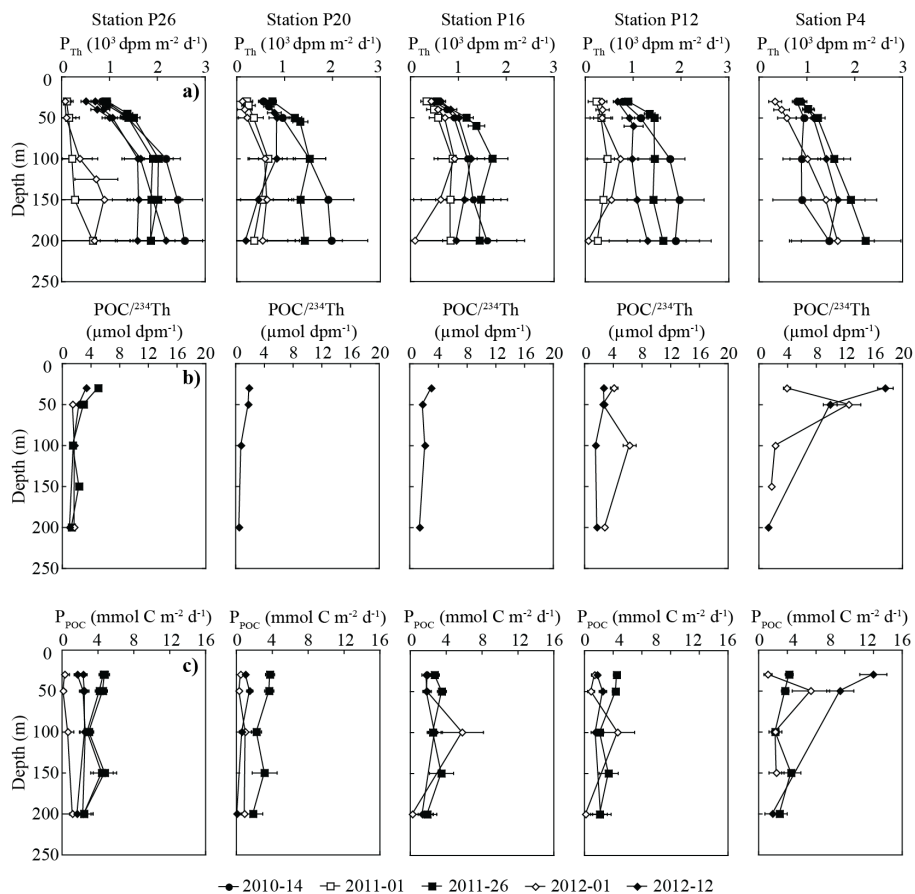


Fig. 9.

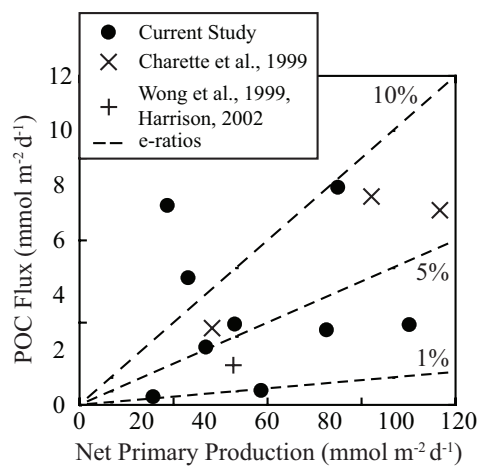
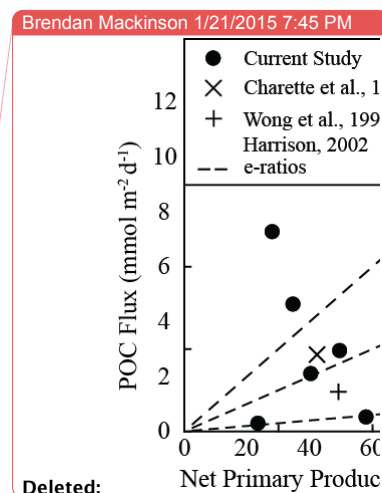


Fig. 10.



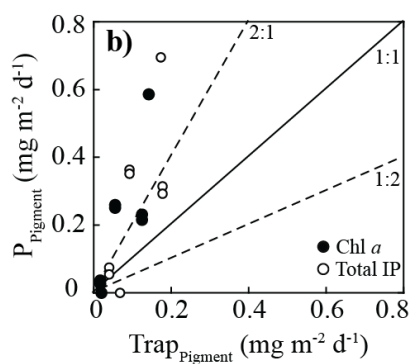
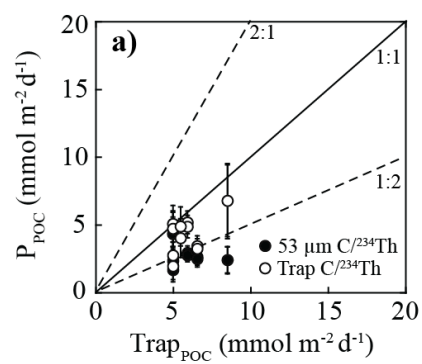


Fig. 11.

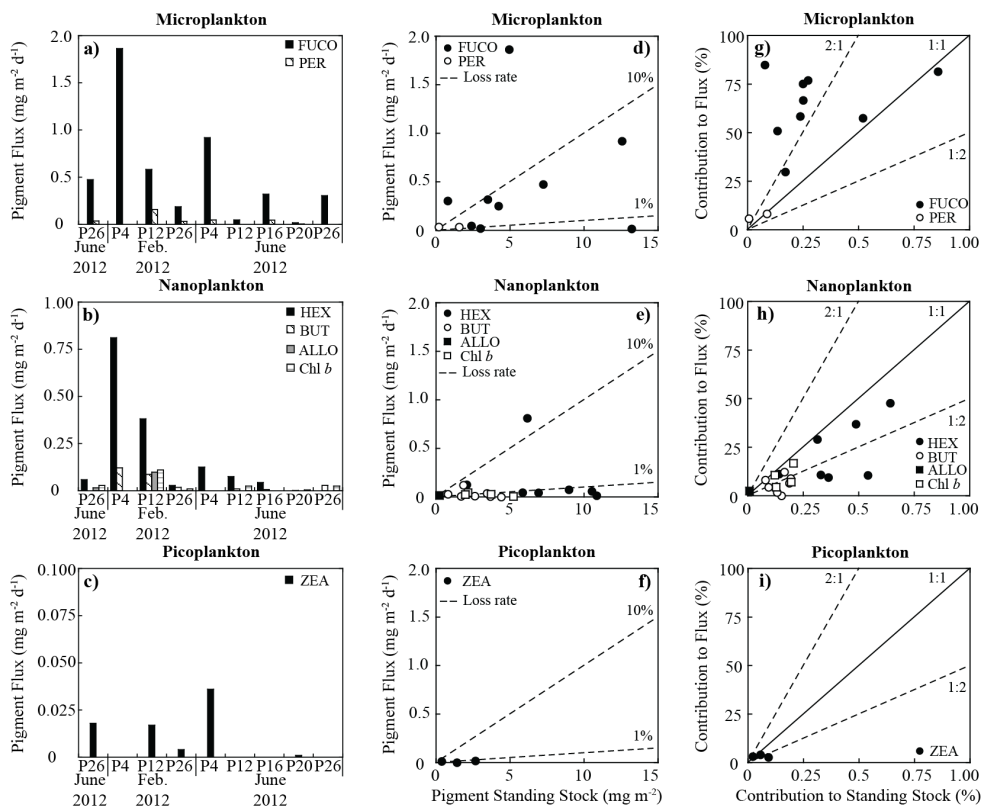


Fig. 12.